A SHORT HISTORY OF MEMBRANE PHYSICS

Erich Sackmann and Avinoam Ben-Shaul

1. INTRODUCTION

A critical step during biological evolution has been the enclosure of biochemical reactions inside vesicles made of semipermeable membranes composed of lipid bilayers or, in the case of archaea bacteria of monolayers of bipolar bola-lipids. Integrating into the membranes light-driven proton pumps with pH dependent activity, such as Bacteriorhodopsin, enabled the reactions to proceed under controlled acidic conditions. The incorporation of these pumps into lipid membranes by hydrophobic peptide sequences is a striking example of nature's ability to transform genetic information into biological nano-machines by making use of basic physicochemical principles of self-assembly, such as the hydrophobic effect. Much of our present understanding of the principles underlying membrane self-assembly and the correlation between membrane structure and functions (such as proton pumping), is based on insights gained by designing sophisticated model systems such as giant vesicles, black lipid membranes (BLM), lipid monolayers and supported membranes. Correlations between the molecular organization of lipid-protein bilayers and their basic biological function were established by comparative studies of artificial and natural membranes. Our main goal in this brief historical survey of membrane physics is to point out how our present understanding of membrane biophysics has evolved through the development of novel experimental tools and theoretical concepts of soft matter physics.

In 1925, comparing the surface area of erythrocytes with the monolayer area formed by spreading their constituents, Gortel and Grendel arrived at the conclusion that the thickness of cell envelopes corresponds to that of a lipid bilayer (1). Ten years later, largely based on the electrical properties of erythrocyte suspensions discovered by K. Fricke and other electro-physiologists, Danielli and Davson suggested that cell envelopes are tri-laminar films composed of a lipid bilayer sandwiched between two layers of protein, as illustrated in Fig. 1a, (2). It took nearly forty years before this picture of the bio-membrane has been independently challenged by more realistic models. In the US, based on thermodynamic considerations pertaining to the strong preferences of ionic groups to be in contact with water, and hydrophobic groups to reside in oil-like environment, Singer and Nicolson proposed their Fluid Mosaic Model, Fig. 1b, (3). This model, generally favored by biologists and thus often referred to as "the standard picture of a bio-membrane", depicts the lipid bilayer as a passive two-dimensional (2D) fluid, enabling lateral mobility of integral and peripheral proteins, as needed to fulfil their biological functions. A second model, the Heterogeneous Shell Model (4), favored by many physicists, attributed a more active role to the lipid matrix, Fig. 1c. This model emphasized the tendency of proteins to assemble in functional micro-domains of specific composition by lateral phase separation that are driven by specific lipid-protein interactions in the multicomponent membrane mixture. The model was suggested by studies of auxotrophs of *E.coli* bacteria which can only grow when phospholipids are added to the nutrition medium. One can thus replace the natural lipids by synthetic lipids with well defined transition temperatures. The experiments showed for the first time that biological membranes can undergo temperature driven phase separation below the lipid chain melting transitions and second, that membrane fluidity enabling lateral diffusion of constituents is indispensable for the division and survival of the cells (4).

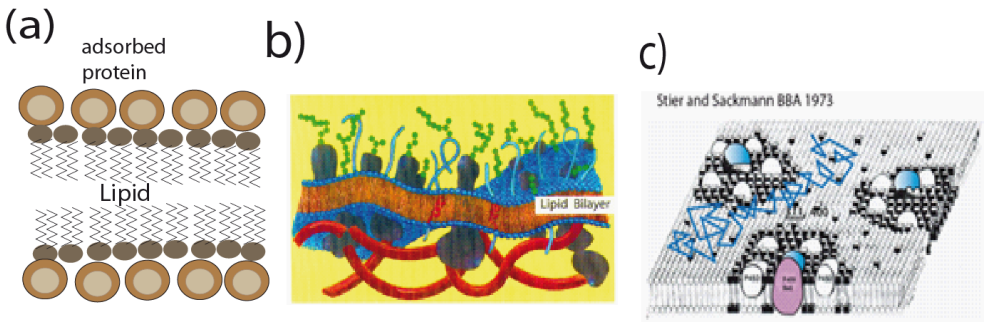

FiIGURE 1 Early models of biological membranes. **(a)** Danielli and Davson model (2). The membrane-associated proteins adsorbed on both surfaces were assumed to control ionic permeability from either side of the lipid bilayer. **(b)** The Fluid Mosaic Model of Singer and Nicholson (3). Lipids are assumed to play a passive role, forming a two-dimensional fluid layer embedding the proteins and enabling their lateral transport. **(c)** The Heterogeneous Shell Model. Lipids play an active role and serve the formation of local functional lipid-protein domains (image reproduced from (4)).

Two groundbreaking developments that have greatly motivated the interest of physicists in membrane biophysics were the Huxley-Hodgkin model of nerve conduction by voltage dependent ion channels, and the discoveries by Luzzati and coworkers in the 1960s and 1970s of the rich and fascinating lyotropic and thermotropic polymorphism of lipid/water systems (5, 6). The complex phase behavior of these systems, and the notion that membranes are two dimensional smectic phases, has naturally attracted the attention of many physicists from the liquid crystal community. Soon afterwards, stimulated by Frank's theory of liquid crystals Helfrich presented his curvature elasticity theory of cell shape changes, relating the splay deformation of smectic liquid crystals to the bending deformation of lipid bilayers (7). Around the same time, many physicists were inspired by Marcel Bessis' wonderful book "The Red Blood Cells" (8). In parallel, electron microcopy and biochemical studies revealed that the red blood cell envelope is a stratified elastic shell made up of the lipid protein bilayer and the associated spectrin-actin network (9) – stimulating the formulation of the composite shell model of cell envelopes (4). Today we know that the spectrin-actin network coupled to the plasma membrane is a universal design principle, stabilizes cell envelopes, e.g., of hair cells in the auditory systems (10).

The development of the black lipid membrane (BLM) technique by P. Mueller, M. Montal and coworkers in 1962 (reviewed in (11)) allowed for the first time systematic studies of the physics of ion translocation across lipid membranes, mediated by ion carriers (e.g. Valinomycin) or through membrane pores formed by the oligomerization of proteins such as gramicidin or Alamethicin, Fig. 2. The subsequent development of voltage jump current relaxation methods and ion current fluctuation spectroscopy provided detailed insights into the kinetics of diffusion-limited formation of ion channels by complex formation of amphiphatic polypeptides (12, 13).

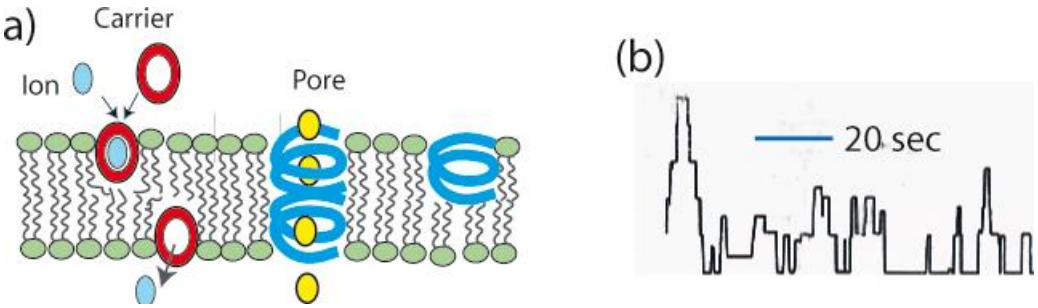

FIGURE 2 **(a)** Schematic view of ion translocation by ion carriers (left) and pore forming amphiphilic peptides, such as Gramicidin (right). **(b)** Current fluctuations through BLM in the presence of small concentrations of gramicidin. The jumps in conductivity increase by constant increments, indicating that one or several channels open simultaneously. Image reproduced from the work of D. Haydon and S. Hladky (11).

Notwithstanding the fading interest in BLM studies, the contribution of this technique to our understanding of the physics of ion translocation through membranes has been enormous. It provided the first experimental proof of the Huxley-Hodgkin postulate of voltage dependent ion channels, paved the way for the interpretation of patch clamp experiments (introduced by Neher and Bert Sakmann), and showed that simple ion carriers, such as Valinomycin exhibit stunning ion selectivity. For instance, the channels formed Alamethicin oligomers were shown to exhibit cation or anion selectivity, depending on the charge of the amino acid side groups facing the channel (12, 13) providing the first experimental proof that the charged amino acids lining the surface of a membrane channel pore determines its ion selectivity. Based on Fourier Spectroscopy of current fluctuations and Voltage Jump Relaxation experiments sophisticated methods for the analysis of ion translocation kinetics through integral membrane channels, or those formed by the assembly of amphiphatic proteins (e.g., Alamethicin) were developed between 1970 and 1980. The simple design of BLM-based systems played a key role in the development of these techniques and the demonstration of their reliability. It thus paved the way for the kinetic analysis of single channel conductivity in cell membranes by the patch clamp technique (reviewed in (14)). BLMs have also been successfully used to study various other fundamental membrane processes, among which are vesicle fusion (15) and the control of ion conductivity by lateral phase separation (16). In the last 20 years the BLM techniques has been widely replaced by solid supported membranes (17), fabricated by deposition of lipid-protein bilayers on solid state devices such as SiO_2 or GaAs based semiconductors. Similar to BLMs these model systems offer many (still unexplored) advantages for studying fundamental membrane properties, such as the fusion of endosomes with model membranes (16).

In the following sections we shall mention various aspects of membrane physics, focusing mainly on the early contributions to each of the topics considered. More recent and modern developments will undoubtedly be described in more detail in other chapters of this volume. Accordingly, we shall briefly discuss some of the early theoretical studies of membrane phase transitions, lipid chain order, lipid-protein interactions and membrane elasticity, yet we shall barely mention the many recent large scale and multi-scale Molecular

Dynamics (MD) simulations of such systems and phenomena. Obviously, we shall not be able to discuss all the many relevant aspects of membrane physics, nor to properly cite all the outstanding studies that contributed to our current understanding of membrane structure and function. We apologize in advance for any unjustified omission of a relevant reference, as well as for our possible personal biases.

2. POLYMORPHYSM OF LIPID-WATER SYSTEMS

In 1968, based on sophisticated X-ray scattering studies Luzzati and coworkers were the first to reveal the rich lyotropic and thermotropic polymorphism of phospholipid-water systems (5, 6, 18). They observed that natural lipids, such as egg lecithin, exhibit similar lyotropic phases to those formed by synthetic surfactants. They also found that lipid bilayers undergo a first order chain melting transition. Since then, numerous experimental and theoretical studies have been reported, extending and enhancing our understanding of lipid-water assemblies and their phase behavior. A few of the early findings are briefly outlined below.

2.1 LYOTROPIC POLYMORPHISM

The lyotropic lipid assemblies of greatest biological relevance are the multi-lamellar (*L*) phase and the cubic (*Q*) phase including its disordered bicontinuous version known as the sponge phase (L_3). Tightly packed multi-layers are present for instance in the nervous system, playing a key role as low capacitance layers in myelin sheath of axons. A unique feature of the *Q*-phase is that its constituent lipid molecules form an ordered 3D network of interconnected, water-filled, bilayers tubes (18). Upon swelling, the cubic symmetry may disappear but the network topology remains intact, resulting in the formation of a the L_3 phase. Interest in this phase increased recently following the discovery by Rapoport and coworkers that the endoplasmatic reticulum can form tubular networks extending throughout the entire cell (19, 20).

The early findings about the polymorphism of lipid-water assemblies indicated the possible role of lipid phase transition in controlling biological membrane processes. For instance, the L_β to L_α transition discussed below, allows cells to adjust the elasticity and fluidity of their membranes in response to changing environmental conditions (21). These notions stimulated the development and application of various new experimental techniques, as well as a burst of theoretical studies. Important insights into the molecular order and dynamics of fluid phases were gained by measurements of lipid orientational order parameters using Deuterium NMR (22, 23), infrared (24) and spin label ESR spectroscopy (25). Chain segment distributions and dynamics were derived by neutron scattering methods (26–28), and correlations between vesicle shape changes and phase transitions were gained by freeze fracture electron microscopy (EM). For review, see reference (29). In parallel, thermodynamic properties could be measured with high precision using dilatometry ((30–32), light scattering, FTIR spectroscopy (21, 30) and sensitive calorimetric methods (33).

2.2 THEMOTROPIC POLYMORPHISM OF LIPID BILAYERS

In addition to the rich polymorphism of lyotropic 3D lipid phases, lipid bilayers exhibit a number of thermotropic phase transitions taking place within the 2D membrane plane. Their number and character are even richer and more intricate in multicomponent lipid bilayer and lipid-protein membranes (18, 29, 34–37). At low temperatures the lipid molecules are immobile, forming a "gel" phase, in which the lipid head groups are generally densely packed, organizing typically in orthorhombic crystalline order. The hydrocarbon lipid tails in the gel phase are stretched, with their main axes parallel to each other and directed either parallel or tilted with respect to the membrane normal, with the respective phases denoted as L_β and $L_{\beta'}$. The $L_{\beta'}$ structure is generally observed in bilayers composed of lipids with large polar head groups, such as phosphatidylcholines, whose cross sectional area is larger than that of their (fully stretched) two-chain hydrocarbon tails. The tilting enables tighter packing of the tails, enhancing chain cohesion within the hydrophobic membrane core.

Below we briefly outline a few of the numerous pioneering experimental and theoretical studies of bilayer phase transitions and lipid order in membranes. Related topics, such as lipid-protein interactions, as well as membrane defects, dynamics and curvature elasticity are discussed in subsequent sections.

2.3 THE $L_\beta \rightarrow L_\alpha$ AND OTHER BILAYER TRANSITIONS

Common to all lipid bilayers is a first order chain melting transition ($L_\beta \rightarrow L_\alpha$) from the gel phase to a 2D fluid phase, taking place at a well-defined temperature T_m. Above this temperature, in the L_α phase, the membrane is a 2D fluid, enabling lateral translation of the lipids in the membrane plane, as well as limited conformational freedom of their flexible hydrocarbon tails. The extent of chain conformational freedom depends sensitively on the cross-sectional area per lipid head group a, whose value depends on the balance of repulsive and attractive inter-lipid forces: The effective attraction between lipid tails which tends minimize the unfavorable surface energy associated with exposing the hydrocarbon region to contact with water, vs. the repulsive forces due electrostatic and excluded volume interactions between head-groups, as well as the entropic repulsion between the hydrocarbon lipid chains in order to increase their conformational freedom. This balance of forces is schematically described in Fig. 4.

Widely varied in their mathematical approaches, most theories of the $L_\beta \rightarrow L_\alpha$ transition agree that its primary thermodynamic driving force is the gain in conformational (trans/gauche) entropy of the hydrocarbon lipid chains above T_m, compensating for the partial loss of cohesive energy of the hydrocarbon chains in the passage to the (~4%) less dense L_α phase. This interplay between inter-chain attraction energy and conformational entropy is reflected in the chain length dependence of T_m . Thus, for example, in the case of bilayers composed of PC lipids with two saturated hydrocarbon tails, T_m increases from 23C to 41C to 55C as the lipid chain length increases from n = 14, to 16 to18 methylene groups, respectively, (29, 36). While both the enthalpy and entropy changes in the transition increase with n, the monotonic (roughly linear) increase of $T_m = \Delta H_m / \Delta S_m$ with n, indicates a stronger chain length dependence of the transition enthalpy. The presence of a double bond

along the hydrocarbon chains has a dramatic effect on the chain-melting transition. Depending on the position of the C=C bond, T_m may be 1°C to 60°C lower upon shifting the position of this bond from the vicinity of the head group to the center of the chain, and then up again by about 50°C when the double bond is close to the chain end, as observed for dioctadecanoyl-PE (C18:1-PC) bilayers (38). A possible explanation to this behavior is that when the double bond is located near the beginning or end of the chain, most of the chain can still behave as a saturated one enabling relatively efficient packing in the gel phase, while its presence in the middle of the chain introduces chain tilting resulting in a perturbation to lipid packing resulting in lower transition temperature.

Among the early theories of the chain melting transition are exact mathematical solutions to approximate bilayer models, e.g., Nagle's dimer model of hydrocarbon chains on a 2D lattice (39), Scott's (40) and Pink's (41) "few-states" chain models, as well as Landau theories using the chain segment density (ρ), the average orientational order parameter (η), or the area per head group (*a*) as the relevant thermodynamic order parameter (42–44). Realistic, albeit approximate, molecular-level theories have also been proposed. First among these is Marcelja's pioneering theory (45, 46), where all rotational isomeric states of the hydrocarbon chains are taken into account, and their interactions and bond orientational order parameters treated in analogy to the Maier-Saupe theory of the isotropic-nematic transition. In addition to the chain melting transition, his theory and subsequent molecular level models, followed by a growing number of increasingly sophisticated and extensive Molecular Dynamics (MD) simulations, have provided detailed information about chain conformational properties in the fluid phase, as discussed in little more detail in Sec. 2.5. Many of these approaches were later extended and applied to analyze the phase behavior of multi-component lipid bilayers and lipid-protein membranes (Sec. 4), and to explain and predict the molecular aspects of membrane elasticity (Sec. 8).

Another topic of physicists' interest has been the phase behavior of the lipid bilayer below T_m (47). While crystalline, the gel phases prevailing at these temperatures are remarkably flexible, resembling the glassy state of polyethylenes. The hydrocarbon chain dynamics in the bilayers involves kink formation and rapid diffusion along the hydrocarbon chains, as discussed in Sec. 6, see Fig. 11. Among the challenging issues pertaining to the crystalline phases is their rich defect structure, which is largely due to the frustration of lipid packing owing to two reasons: First, because the fatty acid chains cannot rotate freely about the carboxyl groups linking them to the head group phosphates (in contrast to ether lipids). Second, because the hydrocarbon chains prefer forming a triangular lattice while the head groups prefer orthorhombic packing, see Fig. 3c. The defect structures associated with these frustrations (29) became popular paradigms for studying the physics of flexible two-dimensional solids such as polymerized membranes. These solids exhibit a novel type of a phase transition with diverging specific heat, termed the *crumpling transition*, which is a consequence of the dissociation of dislocations (48). The spatial long range order of the crystalline lattice of the low temperature phase is lost in this transition, while the long range orientational order (i.e., the orientation of the crystal axes) is maintained. This new type of a solid state is known as the *hexatic phase*. Among others, it was suggested to characterize the structure of the spectrin-actin network of erythrocytes; see e.g., (29).

In many cases, predominantly in membranes composed of lipids with large head groups, the chain melting transition is preceded by a weak, pre-transition, taking place at a

temperature $T_p<T_m$, whereby the bilayer transforms from the crystalline $L_{\beta'}$ phase to a corrugated phase, commonly known as the *ripple phase*, and denoted $P_{\beta'}$ (36, 47). Unravelling the origin of the ripple phase has challenged many experimentalists and theorists. One rather consistent conclusion from the various studies is that the lipids in the long edge of the ripples are densely packed – resembling the $L_{\beta'}$ order, while the shorter edge is thinner and lipid packing there resembles the L_α phase. The theories suggested range from continuum models, through molecular level calculations, to Molecular Dynamics (MD) simulations, yet a full picture is still missing and the nature of the pre-transition is still a matter of controversy. Early models of the ripple phase can be found in (29).. For a recent study and survey of the ripple phase see e.g., (49).

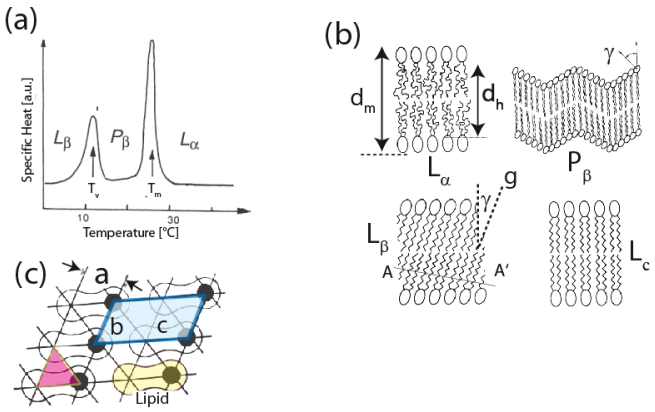

FIGURE 3 **(a)** The heat capacity of a suspension of vesicles of dipalmitoylphosphatidyl-glycerol (DPPG, C:16,0 PG), showing the chain melting transition ($L_\alpha \rightarrow L_\beta$) and the pre-transition ($L_\beta \rightarrow P_{\beta'}$). **(b)** Schematic illustration of the molecular architecture of the fluid (L_α) and three solid phase, ($P_{\beta'}$, L_β and L_c). The non-tilted crystalline L_c-phase forms by annealing the L_β-phase at temperatures below the pre-transition temperature T_P **(c)** The solid phases are frustrated because the head groups favor the orthorhombic symmetry while the chains prefer the triangular lattice (of lattice constant a=0.42 nm).

2.4 LIPID MONOLAYERS

In the early 1970s lipid monolayers were intensively studied as potential model systems of bio-membranes, offering unique possibilities to establish phase diagrams of lipid mixtures as functions of temperature and lateral pressure. Monolayers are also useful to study the nucleation and growth (Ostwald ripening) of micro-domains of lipid mixtures (50–52). Furthermore, monolayer experiments provide direct determinations of the thermal expansivity and compressibility of lipid layers, enabling parallel characterization of their molecular architecture by high resolution X-ray and neutron surface scattering (53).

Lipid monolayers have been extensively used to study the adsorption and enzymatic activity of proteins as a function of the lipid packing density. Striking examples are the cleavage of phospholipids by phospholipases and the exchange of proteins between vesicles of different composition mediated by lipid exchange proteins, showing that enzymatic activity in the fluid-solid coexistence region is far more efficient than in either the fluid or the gel phase (53). Underlying this behavior is the diverging membrane compressibility in the phase transition, enabling the enzyme to efficiently grab lipids in the domain boundaries and

membrane defects accompanying the transition (see Sec. 7). Monolayer studies are also expected to provide important insights into the mechanisms associated with the recruitment of oppositely charged lipids to the vicinity of peripherally bound macromolecules such as proteins or DNA.

2.5 LIPID CHAIN ORDER IN THE L_α PHASE

Information concerning chain ordering and conformational freedom in the (biologically relevant) L_α phase has been the goal of numerous experimental, theoretical, and computer simulation studies. Of particular interest are the orientational bond order parameter profiles of the lipid chains, which are usually provided by Deutrium-NMR measurements (22, 54), and the spatial distributions of lipid chain segments obtained by X-ray and neutron scattering (26, 55, 56). The late 1970s through the 1990s witnessed the appearance of numerous theories and simulation studies of lipid chain order, including elegant lattice models (57, 58), pioneering MD simulations (59), as well as a number of mean field theories (45, 60–62) showing very good agreement with experiment; for a review of the early theories see for example (63).

The orientational bond order profile, $\{S_k\}$, represents the average relative orientations of the C_k-C_{k-1} bonds along the hydrocarbon lipid tails relative to the membrane normal. They are directly related to the C-H bond orientations which can be determined by selective deutration of the C_k-H bond, yielding $S_k = (1/2)\langle 3\cos^2\theta_k - 1\rangle$, where θ_k is the angle between bond C_k-D bond along the hydrocarbon chain and the membrane normal, $\boldsymbol{n}$. The angular brackets denote averaging over all possible chain conformations. In Marcelja's pioneering theory (45) $\{S_k\}$ appears explicitly in the self-consistency equations for the nematic-like molecular field, $\Phi = V_0\left\langle (n_{tr}/n)\sum_k S_k \right\rangle$, with n_{tr}/n denoting the fraction of C-H bonds in *trans* conformation. $V_0 \approx 700\ cal/mole$ was used as the average van der Waals energy per chain in the corresponding polyethylene liquid. His solution, for any given chain length, *n*, yields both $\{S_k\}$ and the average area per head group, *a*, as a function of temperature.

Other molecular field theories (61–63) evaluated the probability distribution of chain conformations based on the "hydrocarbon droplet" assumption, according to which the hydrocarbon segment density within the hydrophobic core is spatially uniform and equal to that in liquid alkanes (64, 65). An explicit expression for $P(\alpha)$ – the probability of finding the lipid chain in conformation of lipid chain conformations α – can be derived (for any given area per lipid head group a) by minimizing the chain free energy subject to the constraint of constant segment density (62, 63).The result is

$$P(\alpha) = \frac{1}{q}\exp\{-[\varepsilon(\alpha) + \int \pi(z)\varphi(\alpha; z)dz]/k_B T\} \qquad (1)$$

where $\varepsilon(\alpha)$ is the chain conformational (e.g., trans/gauche) energy in conformation α, $\varphi(\alpha; z)dz$ is the number of chain segments whose centers in this conformation fall within the layer $z, z+dz$ parallel and at distance z from the hydrocarbon-water interface; k_B is

Boltzmann's constant, and T is the temperature. The $\pi(z)$ are Lagrangian parameters representing the lateral pressure profile (see Fig, 3), evaluated by solving the self-consistency equations: $\langle\varphi(z)\rangle = \sum_\alpha P(\alpha)\varphi(\alpha;z) = \rho(z)$, with $\rho(z) = \rho$ denoting the local chain density in the bilayer core. Given $P(\alpha)$ one can calculate any desired single chain property, e.g., the order parameter profile, as illustrated in Fig. 4. Furthermore, thermodynamic quantities, in the mean field approximation, can be derived using statistical thermodynamic relationships involving the partition function, q, and the lateral pressure profile, $\pi(z)$. Such properties include, lipid-protein interaction free energies and membrane elastic moduli, as briefly mentioned in subsequent sections.

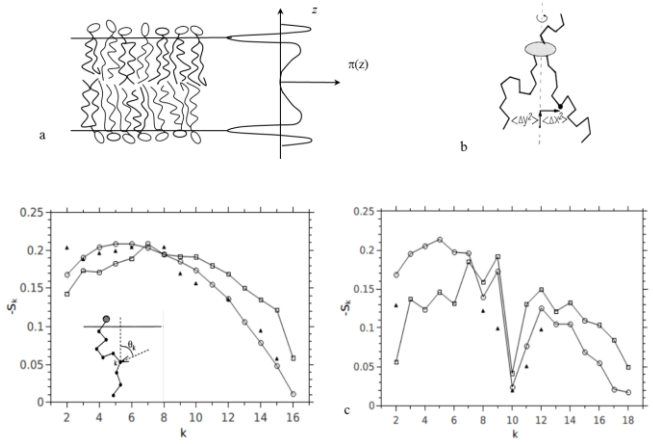

FIGURE 4 **(a)** The lateral pressure profile in a lipid bilayer. Head group repulsion resulting from electrostatic and excluded volume interactions and inter-chain repulsion due to conformational restrictions are balanced by the tendency of the bilayer to minimize water-hydrocarbon contact. **(b)** Characterization of dynamics of chain conformations in terms of mean square displacement of chain segments in horizontal and normal direction (Δx_i^2 Δy_i^2). The local diffusion coefficients in the two directions increases linearly with the distance from the head group. This gradient in segment motion is equivalent to gradient of static order parameter (27). **(c)** Orientational bond order parameters of the C_k-H bonds along the palmitoyl chain (left), and the oleoyl chain (right) of POPC. The palmitoyl chain is fully saturated while the oleoyl chain contains one double bond (between carbons 10 and 11) which perturbs chain order, resulting in the sharp dip in the order parameter profile. The inset illustrate the angles θ_k appearing in the definition of the order parameter. (For an all-trans chain along the membrane normal, $\theta_k = \pi/2$, implying $S_k = -1/2$). The triangles describe the experimental results of Seelig and Waespe-Šarčević (66), the squares are from the molecular dynamics simulations by Heller et al (67), and the circles are from mean field calculations based on Eq. 1 (68).

3. THE LIPIDOME: MEMBRANES AS MULTICOMPONENT LIPID MIXTURES

In the 1970s biochemists began to analyze the complex lipid composition of bio-membranes and to explore the mechanism of lipid synthesis, (see (29, 69) for reviews). Their studies showed that each cell organelle exhibits a characteristic lipid composition which is maintained during the cell's lifetime, despite the rapid exchange of material via endocytosis, exocytosis and intracellular vesicle trafficking. In another series of elegant biochemical experiments the van Deenen group showed that the lipids are asymmetrically distributed between the two leaflets of the erythrocyte plasma membrane: The sphingomyelins (SPHM)

and oligosugar-carrying gangliosides residing only in the outer leaflet, along with phosphatidylcholines (PC). The inner leaflet was found to contain most of the phosphatidylethanolamines (PE) and all the anionic lipids, specifically phosphatidylserines (PS) that comprise about 7% of the acidic membrane lipids, and phosphatidylinositol PI-4,5-P2 comprising about 2% .

Significant differences were also found with respect to the lipid composition of different organelles. Sphingomyelins and oligosugar-carrying gangliosides reside mainly in the PM and the late endosomes, amounting to about 20 % of the total phospholipid content of these organelles, as compared to only 3% -10 % of these lipids in other organelles. Deveaux and coworkers provided evidence that the asymmetric lipid distribution is maintained by specific ATP-dependent translocases called flippases (70). Differences in cholesterol concentrations are also striking; the molar concentration of cholesterol in the nuclear membrane, the endoplasmatic reticulum (ER) and Golgi is less than 10%, as compared to 15% in lysosomes and 42% in the PM which is close to the solubility limit (see Fig. 5b). Steck and coworkers showed that this gradient of cholesterol distribution is actively maintained (71). The fine tuning of lipid homeostasis is mediated by specific exchange proteins, transfering lipids between the outer leaflets of intracellular organelles (see Fig. 12 below).

Correlations between the thermodynamic phase state and the biological function of the membrane became evident following the observation that cells can adapt to the ambient temperature by proper choice of lipid chain length, the fraction of unsaturated lipids and the number of double bonds of these lipids. In particular, specific enzymes were found to help plant cells adjust to low environmental temperatures by increasing the fraction of unsaturated lipids (72).

Taken together, these observations showed that the lipid composition is an intrinsic property of each cell type, that their synthesis is genetically controlled, and that lipid and protein bio-syntheses are closely regulated. In analogy to the terms genome and proteome, we may therefore regard the sets of lipids in the various organelles as the lipidome.

Unravelling the homeostatic control of lipid composition of cell organelles triggered numerous physico-chemical studies of the phase behavior of multi-component lipid and lipid-cholesterol layers. A wealth of experimental techniques were developed for this purpose, including ESR spectroscopy (21, 34), NMR-techniques (34, 73), FTIR- and Raman-spectroscopy (24) differential calorimetry (74), densitometry (75), and Freeze Fracture EM (see (29) for references). All of these techniques determine phase boundaries by scanning the temperature, which means that the lipid composition of the segregated phases changes continuously while scanning through the coexistence region. Therefore, these methods do not allow to determine equilibrium phase diagrams or to directly observe the segregation of phases of equal symmetry, such as solid-solid- or fluid-fluid-immiscibility. At present, Small Angle Neutron Scattering (SANS) in combination with contrast matching, is the only method enabling the establishment of phase diagrams of mixed bilayers of mixed vesicles in thermodynamic equilibrium (76).

An ongoing issue since the early days of membrane physics is whether nature makes use of lipid phase separation in order to maintain the characteristic lipid and protein composition of cellular organelles. Two major questions that arise in this context are (i) why

is cholesterol mainly accumulated in the plasma membrane, and (ii) how are proteins in the plasma membrane recycled during membrane turnover?

Numerous studies on binary lipid-lipid mixtures, ternary lipid-lipid-cholesterol mixtures, in parallel to the search for specific lipid-protein interaction mechanism provided partial answers to these questions. Research along these lines was guided by the expectation that phase separation processes in phospholipid mixtures, liquid crystals and metal alloys are determined by the same thermodynamic concepts, as outlined in the regular solution theory of Hildebrand or the Bragg-Williams lattice models (see (29)). These concepts predicted that, at constant temperature, phase separation is expected to occur if the components exhibit different symmetries (called symmetry rule in liquid crystal physics), or if the molecular shapes of two components (forming the same type of phase) differ remarkably. An example of the first case is the decomposition of DMPC and DPPC mixtures into fluid (L_α) and solid (L_β) phases (fluid-solid demixing). Examples of the second situation are fluid phospholipid-cholesterol mixtures (as shown in Fig. 5b) and fluid mixtures composed of non-saturated PC and PE lipids, as studied by Wu and McConnell (73). A third example are mixtures of saturated lipids differing in chain length by more than two ($n \leq 2$) CH_2 groups, such as DMPC (C14:0-PC) and DSPC (P18:0-PC). This mixture exhibits a peritectic phase diagram with the solid-solid miscibility gap penetrating into the fluid-solid region, resulting in pre-critical phenomena above the liquidus temperature (77, 78).

The phase behavior of binary and ternary mixtures of phospholipids with cholesterol have been the focus of numerous studies. Mixtures of zwitterionic saturated lipids (such as PCs or SPHMs) with cholesterol exhibit phase diagram similar to the one shown in Fig. 5 for the special case of DMPC/cholesterol. SANS experiments showed that, below the chain melting transition ($T < T_m$), this mixture exhibits a miscibility gap between $x_{chol} \approx 0.08$ and $x_{chol} \approx 0.25$. At $x_{chol} < 0.08$ a solid solution is formed, while at $x_{chol} > 0.25$ a homogenous liquid solution of cholesterol in DMPC forms, which saturates at $x_{chol} \approx 0.42$. To fulfil the phase rule the phase line at $x_{chol} \geq 0.25$ is assumed to mark a stoichiometric mixture. Several experiments providing evidence for this interpretation are summarized in (77, 78).

The packing density in the saturated solution ($x_{chol} > 0.2$) is 20% higher than that of the solid solution, It is thus often referred to as a "condensed ordered phase", despite being a 2D fluid. Above T_m there is a fluid-fluid miscibility gap, separating a cholesterol poor expanded phase, L_α, from a cholesterol rich and condensed, yet liquid, phase $L_{\alpha c}$ (where the index c stands for "condensed"). Such fluid-fluid coexistence of phospholipid-cholesterol mixtures was also suggested by theoretical studies (79, 80). The molecular structure and phase changes in lipid-cholesterol systems has been studied in great detail, both experimentally (81), and by molecular dynamics simulations, (82).

The biological relevance of the phase diagram in Fig. 5b becomes evident when we consider the fatty acid chain distribution of membrane lipids (see Table I in (29)). It shows that Sphingomyelins (SPHM) expose mainly long chain lipids with few double bonds (in particular C16:0, C18:0 C24:0 and C24:1), Therefor the natural SPHM fraction exhibits a chain melting transition near physiological temperature, as shown in Fig. 5a (75, 76). In contrast the glycerol based lipids, such as PCs, contain mainly C16:0; C18:0; C18:1; C18:2 and C20:4 and melt well below 10°C. Other notable facts are that cholesterol associates preferentially with saturated lipids (83, 84), and acts as fluidizer of crystalline membranes (29, 76).

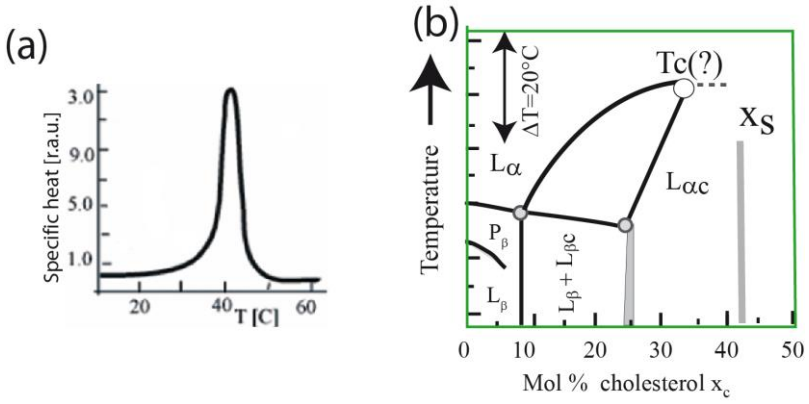

FIGURE 5 **(a)** Demonstration of phase transition of vesicles of brain sphingomyelin (SPHM), reproduced from (85)**. (b**) Phase diagram of a binary mixture of cholesterol and PC lipid, in this example DMPC with T_m=23°C. Below T_m a solid-solid miscibility gap forms which separates two homogeneous low temperature phases described in the text, The vertical bar marks a stoichiometric mixture containing 75% PC. Above T_m two fluid phases coexist. They are separated by a miscibility gap that is expected to end in a critical point at T_c. It separates the cholesterol poor L_a phase and the cholesterol rich condensed L_{ac} phase. Image adapted from (86).

Taken together, these findings suggest that the lipid moiety of mammalian cells can be regarded as quasi-binary mixture composed of glycerol lipid (which melts at T≤ 0°C) and SPHM (with T_m≈40°C). Since the glycerol lipids exhibit a high content of unsaturated fatty acids the cholesterol content (x_{chol}≤10 mole %) and the lipid packing density are small (83). In contrast, the high-melting temperature SPHM fraction is saturated with cholesterol and thus forms a condensed (glass-like) state called $L_{\alpha c}$.

A possible role of the pseudo-binary lipid mixtures for the generation of functional domains in cell membranes and lipid protein sorting became only evident after the establishment of elastic and electrostatic mechanisms of selective lipid protein interaction which will be discussed in the following

4. LIPID-PROTEIN SORTING, INTERACTIONS AND DOMAIN FORMATIONS

Biological functions depend critically on the interaction of the lipid membrane with peripheral and integral proteins, and most often with proteins composed of both hydrophobic and polar domains. The interaction between peripheral proteins and lipid membranes is primarily electrostatic, involving generally attractive forces between polybasic domains and anionic lipids. These interactions will be addressed in the next section, while here we shall comment on the interactions between hydrophobic integral proteins and their surrounding environment of lipid chains.

4.1 LIPID-PROTEIN INTERACTION

The free energy changes associated with the partitioning of polypeptide chains onto the hydrocarbon-water interface of lipid membranes depends sensitively on their length and amino-acid composition. Detailed measurements of interfacial hydrophobicity scales provide

important information pertaining to the folding free energies of the peptides and their propensity to insert into the lipid hydrophobic core (87). While preferring the hydrocarbon lipid chains over the aqueous environment, the presence of a hydrophobic protein inclusion in the membrane core incurs a non-negligible free energy penalty associated with the perturbation of the local lipid order of their surrounding lipid environment. The perturbation energy is proportional to the number of lipid molecules affected by the presence of the integral inclusion, and hence to the circumference of the protein. Indeed, experiments with spin-labelled lipids reveal that the fraction of lipids associated with intramembranous proteins is proportional to their perimeter (88). It also depends on the *hydrophobic mismatch*, $\delta h = h_P - h_L$, which measures the difference between the hydrophobic height of the protein and the thickness of the unperturbed lipid bilayer (89), as illustrated in Fig. 6.

In multi-component lipid membranes the presence of integral inclusions may lead to lipid sorting, attracting lipids of matching height and chemical affinity to their immediate vicinity. Furthermore, in analogy to the hydrophobic interaction – whereby two nonpolar solutes in water are attracted to each other because in contact they cause a lesser perturbation of the water structure around them – the interaction between two hydrophobic inclusions in a lipid membrane is attractive because, together, they perturb a smaller number of neighboring lipids as compared to their being far apart of each other. If the perturbation of lipid order is large enough, as in the case of large $\delta h = h_P - h_L$, the lipid-mediated attraction between proteins can overcome their translational (mixing) entropy, resulting in their 2D condensation to form protein-rich 2D domains.

Treating the lipid-protein membrane as a 2D liquid mixture of N lipids of cross-sectional area a, and N_P proteins of area ga, its free energy in the mean approximation is given by

$$\Delta G_{LP} = Nk_BT\left\{\varphi_L \ln\varphi_L + (1/g)\varphi_P \ln\varphi_P + \chi\varphi_L\varphi_P\right\} \qquad (2)$$

with φ_L and φ_P denoting the area fractions of lipid and proteins, respectively. Proteins whose hydrophobic domain consists of a single α-helix occupy about the same hydrocarbon-water surface area as that of one lipid molecule (typically around 70Å^2) implying g ≈ 1. Larger proteins, such as the band III ion channel, occupy larger membrane areas amounting to as many as g ≈ 20 lipids. As usual, the non-ideality interaction parameter χ is proportional to the difference between the lipid-protein interaction potential and the average of the lipid-lipid and protein-protein potentials. It should be noted, however, that unlike the case of flexible polymers in solutions, integral proteins in membrane are rigid, so that χ depends on their circumference length rather than on their length. The critical point implied by the mixing free energy Eq. 2 is specified by a lower critical protein concentration than that of ordinary ($g=1$) mixtures, namely $\varphi_P^c = 1/(1+\sqrt{g}) \to 1/\sqrt{g}$, and a smaller critical interaction strength, $\chi = (1+\sqrt{g})^2/2g \to 1/2$. Resembling polymer solutions, the binodal curve for large g is strongly skewed, corresponding to very low protein solubility. For example, the solubility limit of Band III at room temperature is $\tilde{\varphi}_P = 10^{-4}$

The strength of lipid-protein interactions can be determined by measuring the shift in the lipid chain melting transition temperature caused by small amounts of membrane proteins, or by the shift of the solidus and liquidus lines (29). Using light scattering and electron

microscopy imaging, Riegler and Möhwald (90) studied the gel-liquid crystal transition of vesicles composed of PC lipids of different chain length containing integral (photosynthesis reaction center) proteins. Consistent with the "mattress model" of Mouritsen and Bloom (89) they found that the lipid mediated attraction between the proteins increases with the magnitude of the hydrophobic mismatch, $\delta h = h_P - h_L$, In parallel, several molecular level models and quite a few continuum elastic theories have been proposed to account for the interactions between membrane inclusions. In 1975, using liquid crystal elasticity theory, Gruler pointed out the changes imposed on membrane curvature due to conical inclusions (91). A year later Marcelja applied his molecular field theory to the case δh=0, where the only perturbation to lipid order is the presence of the rigid protein wall (46). He found that the width of perturbation annulus surrounding an isolated inclusion involves about three lipid diameters. The range of perturbation and its magnitude are larger for nonzero hydrophobic mismatches enhances because lipid the lipid chains adjacent to the inclusion must stretch ($\delta h = h_P - h_L > 0$) or compress ($\delta h < 0$) in order to avoid exposing hydrophobic protein regions to water (92). The lipid-mediated interaction between hydrophobic inclusions has also been studied by quite a few continuum elastic theories. Thus, for example, Schröder (44) predicted that the attraction between inclusions decreases exponentially as a function of their distance R, while Goulian et al (93) found an $1/R^4$ dependence. Safran and coworkers emphasized the importance of the lipid spontaneous curvature, revealing the possible existence of barriers to protein attraction resulting in non-monotonic interaction potentials (94).

In addition to in-plane protein aggregation, the elastic deformation of the lipid bilayer by hydrophobic inclusions can sometimes lead to rather dramatic structural transformations of the lipid-protein matrix. For example, it was found that beyond a certain critical concentration of short hydrophobic peptides ($\delta h < 0$) in a lipid bilayer, a morphological transition of the lipid-peptide mixture can take place from the lamellar (L_α) to the inverse-hexagonal (H_{II}) phase, with the peptides serving as bridges between neighboring water tubes (see e.g., (95, 96)). The critical peptide concentration depends on the spontaneous curvature of the lipids (preferred by lipids with negative spontaneous curvature) and the bending rigidity of the embedding lipid matrix (97). Another well-known peptide-induced morphological transition that has been extensively studied, both experimentally (see e.g., (98, 99)) and theoretically (see e.g., (100–103)) is the formation of membrane pores by amphipathic, anti-microbial, peptides. Similarly, many studies have been concerned with the kinetics and thermodynamics of gramicidin channel formation (100, 101, 104, 105).

Like many other membrane properties, lipid-protein interactions have also been studied using computer simulations, including both MC simulations and especially and in rapidly growing numbers, MD simulations. In recent years, with the advent of fast computers and the development of sophisticated computational algorithms most of the theoretical-computational studies of lipid-protein membranes involve MD simulations. The qualitative insights that have been provided by earlier (both molecular-level and continuum) theory approaches are nevertheless invaluable, especially when large scale cooperative phenomena such as protein-mediated phase transitions, or bio-membrane elastic properties are concerned.

The adsorption of proteins exposing hydrophobic membrane anchors can mediate the formation of local buds by lateral expansion of one monolayer. It has been postulated that such mechanisms of induce budding can trigger the formation of coated pits (86) and caveoli (106).

4.2 LIPID AND PROTEIN SORTING AND THE FORMATION OF FUNCTIONAL MICRO-DOMAINS (RAFTS)

A detailed survey of the length distribution of the hydrophobic thickness of integral proteins residing in the plasma membrane (PM) and the Golgi apparatus due to Bretcher and Munro provided new insights into the physical mechanisms of lipid and protein sorting during membrane turnover by endocytosis and exocytosis (107). They found that the hydrophobic domains of integral proteins (consisting of 15 amino acid residues; $h_P \approx 2.5\,\mathrm{nm}$) in the Golgi apparatus are about 0.5 nm shorter than those present in the plasma membrane ($h_L \approx 3\,\mathrm{nm}$). Together with the selective lipid-protein interaction by hydrophobic matching shown in Fig. 6a, the Munroe Bretcher analysis suggests that protein sorting within the PM as well as between the PM and intracellular organelles could be controlled by lateral phase separation. As illustrated in Fig. 6b, SPHM and the gangliosides reside in the outer leaflet of the PM. Comprising only 12 to 30% of the lipid population in the plasma membrane, SPHM can only cover part of the cell envelope. This suggests that the cholesterol rich SPHM fraction forms lateral domains within the PM which can accommodate proteins with long hydrophobic domains, as illustrated in Fig. 6b. One biologically important example is the Transferrin receptor (29, 108).

This type of domain should not be confused with "rafts", (109). Rafts are generally observed as Triton insoluble membrane fragments and it cannot be excluded yet that they are artefacts generated following the modification of the lipid structure by Triton (108B).

Another case where lipid protein sorting plays a key role is the recycling of receptors after endocytosis by coated pits and caveoli. A well-studied example is the coated vesicle mediated transfer of iron ions into cells via the Fe-carrier transferrin bound to transferrin receptors (reviewed in (86)).

Evidence has been accumulated indicating that some cell surface receptors are directly recycled from the early endosomes to the plasma membrane by the Rab GTPases Rab 4 and Rab 5, thus avoiding the detour about the multibody particles (110). For these special (but vital) cases the lipid protein sorting could be controlled by the phase separation of the S and the glycerol lipid. The transferrin receptor exhibits a particularly long hydrophobic domain ($h_P \approx 4.5\,\mathrm{nm}$ (107)) and could be recycled through the above mechanism. A major step of the recycling is the formation of micro-domains of different curvature by the two segregated phases which grow via Ostwald ripening until the endosomal vesicle becomes unstable and eventually decays into two vesicles, (85, 111). Model membrane studies suggest that fission of vesicles from large endosomes may also by triggered by cholesterol at molar fractions close to the solubility limit of $x_{chol} \approx 0.42$ (85).

The phase separation induced shape changes and vesicle fission is an ongoing theme of membrane physics. It was extensively studied experimentally, first by freeze fracture EM (reviewed in (29) and later by micro-fluorescence techniques (111). Theoretical studies were based on the combination of the bending elasticity model and the Cahn-Hilliard theory of spinodal decomposition (112).

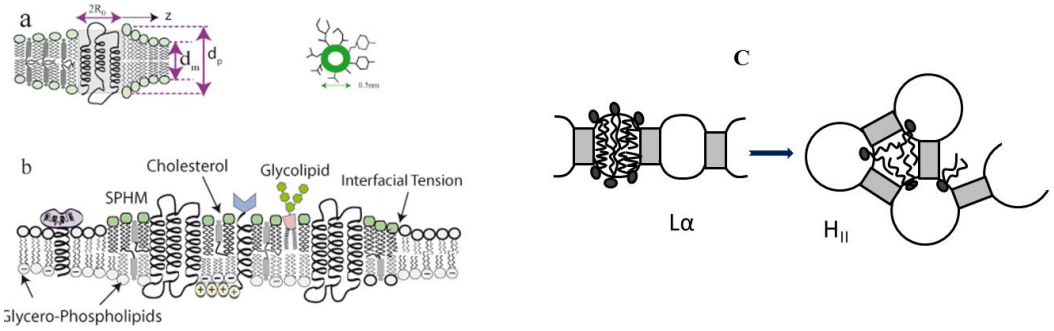

FIGURE 6 **(a)** Elastic distortion of a lipid bilayer induced by the mismatch of the hydrophobic thicknesses of the bilayer (h_L) and the membrane spanning domain of the protein (h_P). **(b)** Model of the plasma membrane suggested by the pseudo-binary phase diagram of Fig. 5 and the Bretcher-Munroe analysis of hydrophobic length distribution of proteins (107). The membrane spanning parts of band III comprises 25 amino acid residues ($h_P \approx 3.8$ nm) and is expected to be surrounded in the outer monolayer primarily by SPHM with C24:0 chains and PE or PC with C18: 0 chains. The cholesterol is expected to accumulate in the outer leaflet. **(c)** Above a threshold concentration of short peptides ($h_P < h_L$) in a bilayer containing long lipids and/or lipids with negative spontaneous curvature, a transition takes place to the inverted hexagonal phase, allowing more conformational freedom to the long lipid chains.

Unfortunately, the interest in the homeostasis of membrane lipid composition and the physics of structure formation by specific lipid-protein interactions has faded considerably in recent years, perhaps because these are very complex fields of research. We must remember however that proper physiological function of cells and hence our health depend critically on the control of lipid and membrane protein patterns. Diseases are often associated with dysfunctions of the lipidome. Thus, for example, erythrocytes of patients suffering from diabetes exhibit a 1-2 mole% higher cholesterol content than those of healthy people, indicating a correlated metabolic disorder. The higher cholesterol content reduces the erythrocytes deformability and could possibly result in blood flow dysfunction.

5. MEMBRANES AS ELECTRIFIED INTERFACES: ELECTROSTATIC SWITCHING OF FUNCTIONAL PROTEINS

The electrical surface potential of biomembranes is dictated by two contributions: First, the presence of about 10% of charged lipids exposing their acidic head groups to the cytoplasmic surface. Second, the electric dipole layer formed by the carboxyl groups of the glycerol backbone, which is located about 0.5 nm below the lipid-water interface (reviewed in (29)). The 2D density and spatial distribution of surface charges affects the structure and thermodynamics of isolated membranes, and plays a crucial role in the recruitment, binding and activation of functional proteins with polybasic domains, as discussed below.

5.1 ROLE OF LIPID CHARGE ON THE CHAIN MELTING TRANSITION

One of the first questions that fascinated physicists has been concerned with the influence of the lateral interaction between charged lipid head groups the gel to liquid crystal transition

temperature, T_m. As first shown by Träuble and Eibl (113) and further elaborated by Jähnig (114)), the surface lateral pressure associated with the electrical double layer, π_{el}, can be regulated by varying the pH or the ionic strength of the embedding solution. The corresponding shift in transition temperature is given by

$$\delta T_m = \frac{\Delta F_{el}}{\Delta S} \approx -\frac{\Delta A}{\Delta S}\pi_{el} \qquad (3)$$

where $\pi_{el} = -\partial F_{el} / \partial A$ with ΔF_{el} denoting the excess electrostatic free energy of the charged membrane relative to the neutral one, with ΔS and ΔA denting the changes in molar entropy and molar area in the chain melting transition, both of which are positive. The transition temperature of the charged membrane is lower because the electrostatic pressure which tends to increase the area per molecule favors the more expanded fluid state, thus enhances the transition.

Application of the classical Gouy-Chapman-Overbeek theory of electrical double layers led to important quantitative relationships between the change in transition temperature and the degree of dissociation of the lipid head groups. Theories developed by Jähnig (114) and others (as discussed in detail by Cevc (115) and Andelman (116, 117)) enabled the calculation of the surface pH as a function of the electrostatic surface potential and the ionic strength of the aqueous phase. An important consequence of the negative membrane surface charge revealed by these early studies is the lowering of the surface pH, which plays a key role in controlling the degree of dissociation of lipids and adsorbed proteins, (118). At low ionic strengths ($I \leq 100$ mM) the effect can be dramatic, inducing significant pH-shifts; $\Delta\text{pH} \geq 2$, (29). The effects are however small at physiological ionic strengths of $I \approx 400$ mM, explaining the fading interest in electrically induced phase transitions.

The electrostatic interactions between lipid membranes containing charged lipids and oppositely charged macromolecules (such as proteins exposing polybasic sequences or DNA) are of great biological relevance. Many of the early studies of these interactions have focused on the calcium induced membrane binding of annexin to PS containing membranes (119). Other early studies demonstrated the charge induced switching of protein function. One intriguing example is the electrostatic switching of the orientation of amphiphatic helices exposing charged head groups in pH-dependent manner from an horizontally adsorbed state into a membrane spanning state, whereby peptides oligomers organize into ion channels, enabling their function as antimicrobial peptides (120).

The interest in electrostatic membrane-protein interaction increased dramatically in recent years following the discovery that acidic lipids, in particular phosphoinositides (PI), such as PI-4,5-P2 and PI-3,4,5-P3, play a key role in the activation of many of the proteins involved in signal transmission across membranes, and the coupling of the actin cortex to the plasma membrane. These, electrostatically switchable proteins contain polybasic sequences comprising up to about 10 basic residues (generally lysines) and post-translationally coupled fatty acid chains (see Figs. 7 and 8).

In the resting state of cells these proteins reside in a sleeping conformation within the cytoplasm, hiding their charged residues and fatty acids. They are activated by exposing their membrane binding sequences (for instance through phosphorylation) resulting in their electrostatic-hydrophobic binding to the membrane surface, as illustrated in Fig. 7. Important examples are the molecular switches of the GTPase family and their associated helper

proteins, such as GTP exchange proteins (GEF) which activate the GTPases by replacing GDP by GTP. The GTPases can be switched-on either directly by the electrostatic hydrophobic binding (as in the case of the Ras-proteins in Fig. 7a), or indirectly by coupling to the membrane anchored GEF. The active GTPase attracts and triggers the function of one or several enzymes; e.g., kinases.

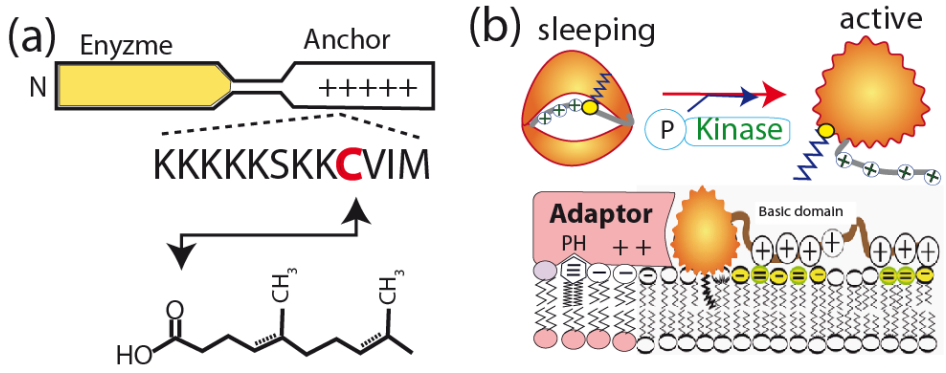

FIGURE 7 **(a)** Domain of structure of the Ras-proteins p21Ras (K-RAS) as a paradigm of protein activation by recruitment to membranes through electrostatic hydrophobic forces. The Ras-protein family consists of a variable domain at the C-terminus containing the polybasic domain and the functional N-terminus. Note that the sequence of lysine groups (K) is interrupted by a polar serine group (S) which can be negatively charged by phosphorylation (see example of MARCKS). The cysteine group (C) is attached to a fatty acid serving as a hydrophobic anchor. **(b)** Enzyme activation by electrostatic-hydrophobic switching. The protein (shown at the top) is activated by phosphorylation, resulting in the exposure of fatty acid anchors and polybasic peptide sequences followed by binding to the membrane by electrostatic and hydrophobic forces. It acts as switch that recruits and activates specific adaptor proteins which in turn attract and activate proteins involved in signal transduction (see also (121)).

The delicate balance of forces underlying the physics of the electrostatic-hydrophobic membrane recruitment of natural proteins has been first systematically explored by McLaughlin and coworkers (122–124) who studied the binding of the Myristoylated Alalnine-Rich C-Kinase Substrate (MARCKS) protein to partially charged membranes. MARCKS – serving as a paradigm of proteins recruited to membranes by electrostatic-hydrophobic forces – consists of a polybasic "effector" domain (ED) containing 13 lysine residues and four intercalated serine groups. The ED is flanked by two flexible chains, both comprising ~150 amino acid residues. The N-terminus flexible domain ends with myristoyl anchor (see Fig. 8b). Similar to the case of K-Ras binding described in Fig, 7, the membrane binding free energy of MARCKS involves a subtle interplay between: (i) the electrostatic attraction of the basic domains to acidic lipids, ΔF_{el}, which provides the major contribution to the binding free energy (ii) the hydrophobic force due to the fatty acid anchor, ΔF_{tail}, and (iii) the entropic free energy loss associated with the flexible – intrinsically unfolded – amino acid chains extending into the aqueous phase, ΔF_{loops}. ΔF_{tail} can be estimated by the empirical law $\Delta F_{tail} = (11-3n)kJM^{-1}$ (29) or from measurements of unbinding forces by single molecule force spectroscopy (125, 126). The electrostatic binding free energy of the effector domain and the entropy loss of the flexible chain extending into the cytoplasm were estimated by MC studies (127).

Consistent with experiment and theory, efficient binding of the basic domain requires the colocalization of a matching number (namely, 13) of acidic lipid charges to the small ED-membrane contact zone. Importantly, most of the protein charge neutralization is achieved through the recruitment of the polyvalent PI-4,5-P2 lipid (generally carrying a charge of -3 or -5) which comprises only ~2 % of the membrane lipids (as compared to 10-30% of the monovalent PS) (123, 127–129). MARCKS-membrane interaction is just one of many examples of the very strong and selective binding of functional proteins to phophoinositides (PI-4,5-P2 and PI-3,4,5-P3). Such binding is generally mediated by specific protein homology domains. Important examples, besides pleckstrin homology domains, are the C1 and C2 domains. The former harbors specific binding pockets for phosphoinositides while the C-domains penetrate the lipid layer with two hydrophobic loops (130). The binding of the C2 domain is calcium dependent.

A possible role of MARCKS is to prevent the unwanted membrane recruitment and activation of enzymes (such as phospholipases) by inducing the segregation of the phosphoinositides and their shielding from enzymatic attack. Indeed, about 10 μM of MARCKS suffices to inhibit the phopholipase Cγ mediated generation of the second messengers diacylglycerol (DAG) and inositol triphosphate (IP3). The electrostatically induced segregation of charged lipids by basic polypeptide sequences such a polylysine has indeed been demonstrated earlier (131).

The screening of the PI-4,5-P2 lipids is abolished by phosphorylation of MARCKS through protein kinase C (PKC), resulting in their unbinding from the membrane. The exposure of PI-4,5-P2 then enables the activation of molecular switches (such as GTPases) following the schemes illustrated in Figs. 7 and 8. One important example is the generation of the specific anchor PI-3,4,5-P3 by phosphoinositol triphosphate- kinase (PI3K) shown in Fig, 8c. PI-3,4,5-P3 acts as a second messenger which strongly enforces the specific binding of molecular switches of the GTPase family or of the phospholipase-Cγ which generates the lipid anchor diacylglycerol (DAG). Since DAG mediates the membrane binding and activation of protein kinase C the protective shield of MARCKS can be rapidly displaced to expose PI-4,5-P2.

A vital role of MARCKS has been established recently. Together with protein kinase C, MARCKS plays a key role for the plasticity of synapses, by enabling the rapid remodeling of dendritic spines at the tip of axons. Knock-out of its gene is lethal (132).

In summary, numerous vital membrane based processes, associated with the restructuring of the actin cortex, such a cell locomotion and cell adhesion, are controlled by the recruitment of actin binding proteins to the cytoplasmic leaflet through electrostatic-hydophobic forces. These proteins swim in the cytoplasmic space in a sleeping conformation and are recruited to specific sites at the cell envelope in a logistic way by external cues, such as cytokines or hormones. Most important is the very strong selective binding to the PI-3,4,5-P3 lipids by the specific binding pockets other than pleckstrin homology domains (130, 133), such as the C2.domain mentioned above . In this way the functional protein, may selectively bind to PI-3,4,5-P3 although this lipid anchor is by a factor 100 less abundant than PI-4,5-P2.

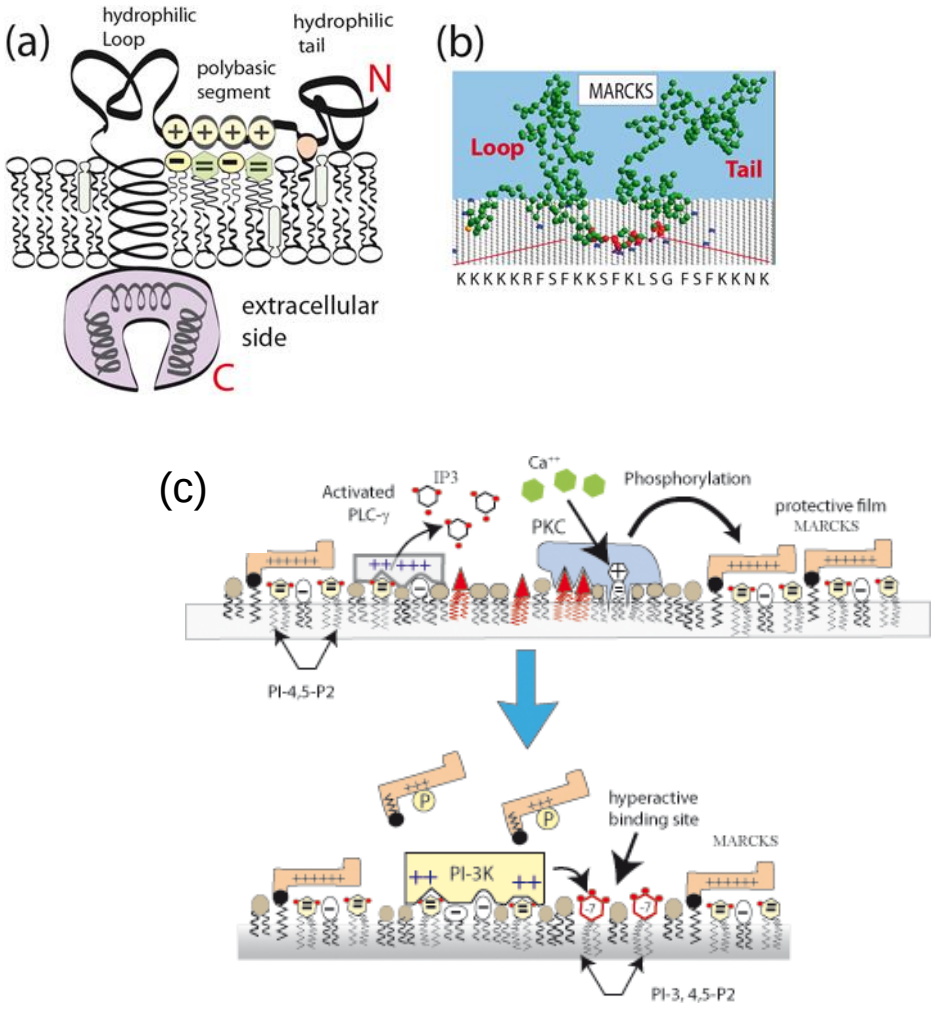

FIGURE 8 **(a)**: Left image: schematic illustration of protein binding to membranes by hydrophobic-electrostatic forces. **(b)** Snapshot from a Monte-Carlo simulation of MARCKS adsorption, showing the enrichment of the binding region by polyvalent acidic lipids (purple), and the hydrophobic binding of the myristoyl anchor at the N terminus (127). **(c)** Possible control of the access of the MARCKS covered phosphoinositides by functional proteins through protein kinase C (PKC) mediated unbinding of the protective layer of MARCKS (shown on the right side). PKC is activated by local bursts of Ca^{++} and DAG-anchors, which are generated by phospholipase Cγ (PLC-Cγ). The activated PKC phosphorylates the serine groups of MARCKS resulting in the explosive displacement of the protective MARCKs layer and the exposure of PI-4,5-anchors. The right side shows the membrane recruitment and activation of the PI-3, 4, 5-P3 generating protein PI-3K kinase (PI-3K). It generates a burst of the highly selective lipid anchor PI-3, 4,5-P2 which enhances the membrane recruitment of many functional proteins, including PLC-Cγ and PI-3K. Please note that in the absence of MARCKS the lipid anchor generators PLC-Cγ and PI-3K would be constantly active, which could result in the over-excitation of cells.

.

5.2. UNDERLYING THERMODYNAMICS AND KINETICS

Two kinds of entropy play principal roles in the electrostatic binding of peripheral "macroions" such as proteins, DNA and other biopolymers to lipid membranes. The first, common to the attraction between any two oppositely charged macroions, is the gain in 3D translational entropy of the mobile counterions originally surrounding the isolated macroions upon their release to the bulk solution; see Sec. 5.4. The second is loss of 2D translational

("demixing") entropy of the oppositely mobile "counter-lipids" upon their migration and segregation near the macroion binding site in order to balance its charge, thus enhancing its membrane binding. In the abovementioned case of MARCKS adsorption, the neutralization of its basic ED is primarily due to preferential sequestration of the polyvalent PI-4.5-P2, whose clustering involves a significantly smaller entropy loss in comparison to that of monovalent acidic lipids (127, 128).

In parallel to the thermodynamic analyses of the electrostatic-hydrophobic protein binding, the dynamics of this process has also been studied, both experimentally and theoretically. Fluorescence correlation spectroscopy measurements revealed that peptide diffusion on the surface of membranes containing PI-4,5-P2 is significantly slower than on those containing only monovalent lipids. It was also found that PI-4.5-P2 diffusion is substantially hampered (129), indicating correlated diffusion of the peptide and the multivalent counter-lipids. Theoretical modeling combining Cahn-Hilliard theory to describe the diffusion of lipid components in the inhomogeneous peptide-dressed membrane, and MC simulations to model peptide diffusion provide further insights into the coupled peptide-lipid diffusion dynamics. Specifically, strongly attracted by the electro-chemical potential gradient due to the peripheral peptide the PI-4.5-P2 lipids rapidly diffuse toward the interaction zone, while monovalent lipids are too slow to follow the motion of the peptide. Further, the relatively strong, albeit reversible, binding of the multivalent lipids to the adsorbing peptides introduces an effective drag that slows down the diffusion of this "complex" (134).

5.3. MACROION AGGREGATION ON THE MEMBRANE SURFACE

In analogy to the lipid-mediated aggregation of integral proteins, the perturbation of lipid organization by peripherally bound macroions can lead to their 2D aggregation on the membrane surface (131, 135). The underlying driving forces are quite different however. One interesting case is that of proteins adsorbing onto a membrane composed of a non-ideal, yet sub-critical, binary lipid mixture of charged and neutral lipids. That is, the non-ideality interaction parameter of the lipid mixture (corresponding to χ in Eq. 2, for the case g=1) is not large enough to induce phase separation of the mixture. However, when macroions adsorb onto the membrane surface they attract oppositely charged lipids to their binding zone, resulting in the formation of small membrane patches rich in charged lipids, as illustrated in Fig. 9. Each of these patches involves a line energy proportional to $n\chi$, where n is the number of inter-lipid contacts at the perimeter of the segregated lipid patch (136). To avoid the unfavorable line energy of the macroions-lipid patches, they attract each other with an effective attraction energy of order $n\chi$, which can lead to 2D phase separation of the dressed membrane into macroion rich and poor phases, as illustrated in the bottom panel of Fig. 9.

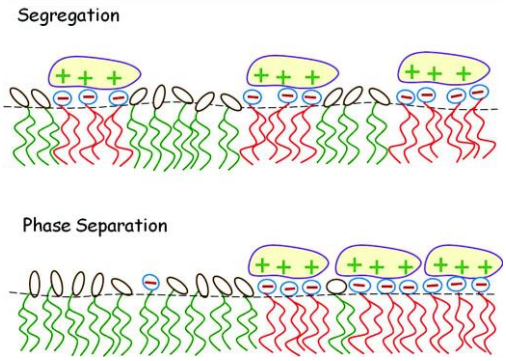

FIGURE 9 Adsorbed macroions attract counterlipids to the interaction zone (top). On non-ideal lipid mixtures this can induce lateral phase separation of the macroion dressed membrane (bottom).

Interestingly, under certain conditions the adsorption of macroions onto oppositely charged membranes can result in charge inversion of the membrane. Namely the net surface charge of the dressed membrane is of opposite sign to that of the bare membrane. This charge inversion (or charge inversion) phenomena is commonplace in polyelectrolyte adsorption onto surfaces, as well as in several cases involving biological molecules, e.g., the charge inversion of DNA saturated by bound polyvalent cations (137). Analogously, when charge inversion is expected when globular basic proteins bind to acidic lipid layers (138), or when DNA adsorbs onto a lipid membrane containing cationic lipids. Charge inversion may also take place upon the adsorption of intrinsically disordered proteins onto lipid membranes. While not impossible, we are not aware of any specific membrane-protein system where charge inversion has been demonstrated experimentally.

5.4. COUNTERION RELEASE

Charged proteins, charged membranes, DNA and other macroions are surrounded by clouds of mobile, generally monovalent, counterions whose confinement to these clouds involves an unfavorable loss of translational entropy. When a charged protein approaches a membrane containing oppositely charge lipids the mobile counterions originally surrounding the macroions are no longer needed because charge neutralization can be provided by counter-lipids; especially so in the case of fluid membranes where the counter-lipids can diffuse and segregate in the protein adsorption zone to provide efficient charge matching, as in Fig. 9. The mobile counterions can now be released into the bulk solution, providing a major, in some cases the principal, contribution to the electrostatic free energy of macroion-membrane binding. The magnitude of the entropy associated with the release of the mobile counterions diminishes upon increasing the salt concentration in solution, consistent with the well known fact that protein-membrane binding weakens at elevated levels of salt in the aqueous solution. The counterion release mechanism has been demonstrated in protein-DNA binding (139), and various other systems (140). A rather dramatic example of the counterion release mechanism is the formation of “lipoplexes” – those spontaneously formed complexes of cationic lipid membranes and DNA (141–143) – as illustrated schematically in Fig. 10a. Conductivity measurements and Poisson-Boltzmann theory calculations suggest that in cases where the

cationic membrane charge density matches the charge density of DNA the entropic contribution to the binding free energy may be as high as ~95%, corresponding to the release of practically all the initially immobile counterions, Fig. 10b (144).

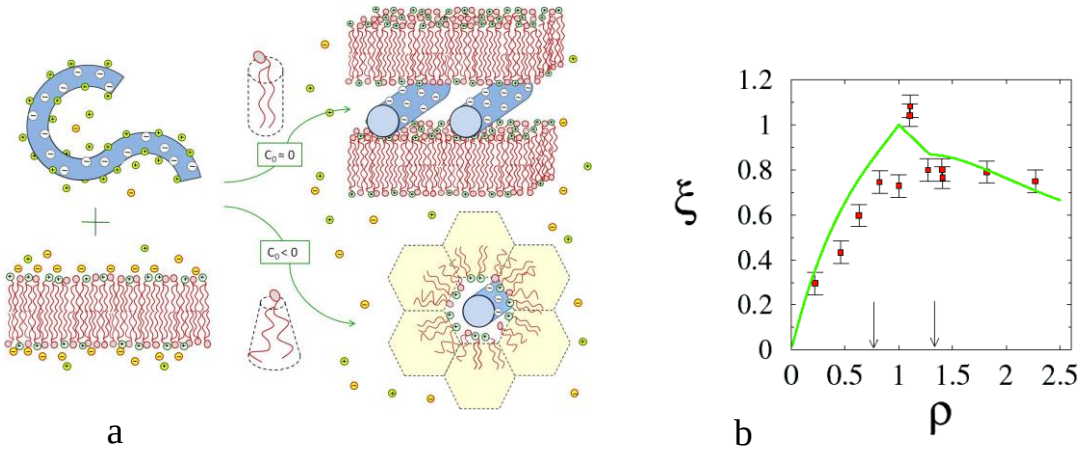

FIGURE 10 **(a)** Schematic illustration of the counterion release mechanism in the formation of DNA–cationic-lipid complexes. The entropy gained by the released mobile counterions provides a major contribution to the complexation free energy. The topology of the lipoplexes formed depends on the spontaneous curvature of the lipids. They are lamellar when the spontaneous curvature is small, and inverse-hexagonal when the lipid bilayers used contain negative-curvature loving ("helper") lipids like PE (145)**. (b)** The fraction of counterions released to solution in the formation of lamellar lipoplexes, reaching a maximum when the charge density on the DNA and the lipid membranes are equal in magnitude, (144).

6. MEMBRANE DYNAMICS: LIPID LATERAL DIFFUSION AND ITS IMPACT

In a pioneering study on membrane dynamics published in 1970, Hermann Träuble (146) showed that water permeability of membrane is driven by the diffusion of gauche-trans-gauche (gtg) kink chain defects along the hydrocarbon fatty acid chains, see Fig.11a. In the same year Frye and Edidin reported the first experimental evidence of lateral mobility of proteins in cell envelopes (147). Soon afterwards, by analyzing the ESR line narrowing due to spin-spin exchange of spin labelled lipids, Träuble and Sackmann provided the first direct data about the lateral diffusion of lipids in membranes, finding $D_{lat} \approx 1\text{-}10^{-12}$ m^2/sec for the lateral diffusion coefficients of (148). Around the same time evidence for the high lateral lipid mobility has also been demonstrated by NMR spectroscopy (149). Later on, short range diffusion coefficients (over ~100 nm) were derived by analyzing the kinetics of excimer formation and subsequent fluorescence following collisions between pyrene labelled lipids (150). The application of this method to lipid cholesterol mixtures led to the development of the free area model of molecular diffusion in membranes. This model accounts for the fact that (unlike in solids) molecular diffusion in liquids is not an activated process but rather driven by density fluctuations in the liquid. Nevertheless, the diffusivity in the membrane obeys an Arrhenius-like law, where the temperature dependence of D_{lat} is dictated by the thermal expansivity of the fluid, (150). The quantitative analysis of measurements of diffusion

coefficients in phospholipid cholesterol mixtures by this model provided one of the first experimental proofs of the condensing effect of cholesterol. The model was extended by Almeida and Vaz (151) and Saxton (152) and applied to explore the membrane heterogeneity by Monte Carlo Studies.

The next technical advancement arrived with the development of single molecule tracking techniques which were developed following the invention of high sensitivity CCD cameras, and enabled measuring the time dependence of the mean square displacement of single lipids or proteins, $\left\langle \left| x(t) - x(t+\tau) \right|^2 \right\rangle = A\tau^{ß}$. Deviations from the random walk model ($\beta = 1$) yielded new insights into the heterogeneous organization of cell membranes (153). Additional new and attractive perspectives opened up following the development of the fluorescence correlation spectroscopy (FCS) technique, pioneered by the group of Webb (reviewed in (154)). By analyzing the temporal correlation function of fluorescence signals FCS enables to distinguish between lateral motional processes and chemical reactions in nanometer size areas. Among the early applications of this method is the abovementioned measurement of the on-off-kinetics of the binding of the MARCKS protein to charged vesicles by electro-hydrophobic forces (155).

Lateral diffusion became most prominent among physicists following the seminal work of Saffman and Delbrück who showed that D_{lat} depends only logarithmically on the radius of integral (156). This law implies that large objects diffuse nearly as fast as lipids, rendering diffusion limited enzyme reaction in membranes very efficient. This is another beautiful example demonstrating how smart nature is in using physical principles to advance biological processes.

The Saffmann-Delbrück model was later extended by Evans and Sackmann to more realistic situations were integral proteins interact weakly with their environment, e.g., through the frictional coupling of membrane proteins to the actin cytoskeleton or the diffusion of proteins in supported membrane (157). Using Einstein's relationship between the diffusion (D_{lat}) and the frictional (λ) coefficients, $D = k_B T / \lambda$, the model proved useful in measuring the friction coefficient between juxtaposed monolayers of supported membranes, or between integral proteins in supported membrane and the solid surface. In the case of large frictional coupling of an integral protein (of radius R) with the surface, the diffusion coefficient becomes: $D_{lat} = k_B T / \pi b_c R^2$, where $b_c = \eta_w / H$; η_w denoting the frictional coefficient of the fluid layer and H is the distance between the protein and the surface (157, 158). Recent progress was made by Komura et al who studied the diffusion of proteins in membrane coupled to viscoelastic media (159). Their model opens new possibilities to explore the impediment of membrane protein diffusion by frictional coupling of the extrinsic domains to the actin cytoskeleton or the glycocalix.

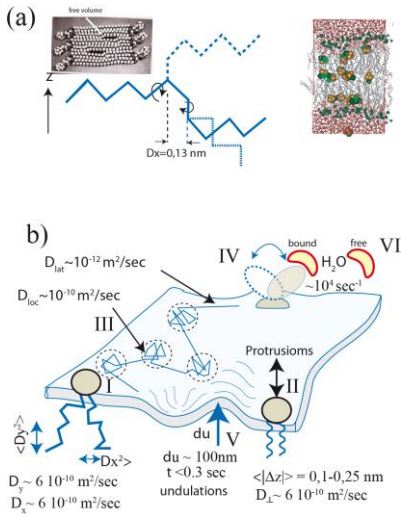

FIGURE 11 **(a)** Left: model of gtg-kink diffusion. Simultaneous hindered rotations about two C-C bonds (separated by one C-C bond) enable the kink performing diffusional jumps of length $\Delta L \approx 0.13$ nm. The jump frequency of $\nu_j \approx 10^{-11}$ sec^{-1} corresponds to kink diffusivity of $D_{kink} \approx 10^{-5}$ cm^2 sec^{-1}. Right: snapshot of membrane as observed by MD calculations. The clusters of yellow and green beads indicate molecules of the anesthetics halothane, demonstrating the role of the hydrocarbon chain region as an apolar organic solvent of small hydrophobic solutes (image reproduced from reference (160)) with permission of the authors. **(b)** Summary of membrane dynamics from the nanosecond to the ten second time regime as revealed by QENS and NMR or ESR relaxation experiments.

The most versatile technique for measuring molecular motions in model membranes is quasi-elastic neutron scattering (QENS). Owing to spin-spin exchange between spins of equal quantum number (S=±1/2) the neutron scattering function of protonated material is incoherent (the scattering length density becomes negative). This unique feature allows us to analyze the motion of single lipid molecules (or portions thereof) by embedding fully (or partially) protonated lipid molecules in a bilayers of fully deuterated lipids. The incoherent scattering provides information on the single proton self correlation function

$$G^{inc}(|\vec{r}-\vec{r}'|,t) = \left\langle \sum_i \delta(\vec{r}'-\vec{R}_i(0)\ \delta(\vec{r}-\vec{R}_i(t)\right\rangle - \left\langle n^2 \right\rangle \qquad (4)$$

By studying oriented lipid multilayers one can determine the direction of lipid motion with respect to the membrane normal. If the motion is unlimited $G^{inc}(|\vec{r}-\vec{r}'|, t)$ decays to zero for $t \to \infty$. In contrast, the self correlation function reaches a finite value G_∞ if the motion is restricted. G_∞ is called the elastic incoherent scattering factor (EISF). EISF measurements yield quantitative information on the lateral extent of the motion of molecules or of molecular segments. Application of different QENS instruments enable studying molecular motions in the time range of 10^{-7} to 10^{-9} sec. By combining QENS with NMR the dynamic range can be extended to 1Hz.

Several important new insights about membrane dynamics that were provided by QENS are depicted in Fig. 11. These are:
(i) The lipid lateral diffusion involves fast local motions ($D_{loc} \approx 10^{-10}$ m^{2}s^{-1}) and long range lateral motion ($D_{lat} \approx 10^{-12}$ m^{2}s^{-1}), in agreement with the free area model of lateral diffusion.
(ii) In the course of the $L_\beta \rightarrow L_\alpha$ transition the number and mobility of chain defects increase continuously whereas only long wavelength motions with Q < 1.9A^{-1} (or $\Lambda \geq 3$ A) show a

discontinuity at T_m. (iii) The dynamic range of QENS ($10^{-13}<\nu<10^{-8}$) can be extended to the millisecond time range by the combination of QENS and NMR relaxation experiments, providing new insights into the local motions of the water molecules bound to lipid head groups (161). (iv) Measurements of out of plane motions of single lipids support the mechanism of short range protrusion fluctuations suggested by Israelachvili and Wennerström (65, 162).

7. MEMBRANE DEFECTS: PHYSICS AND BIOLOGICAL FUNCTION

The role of chain defects in fluid liquid crystalline bilayers has been an ongoing theme since the early 1970s (see). In natural membranes, defects can come into play in various ways. The transport of water across membranes and the diffusion of small hydrophobic molecules (such as local anesthetics) within membrane by kink diffusion are among the examples. Chain packing defects are likely to form in highly curved bilayers and at the rim of SPHM rich micro-domains (see Fig. 6). The detailed analysis of the topology of defect structures of vesicles by freeze fracture EM showed for the first time that tilted phases, such as the $P_{\beta'}$ and the $L_{\beta'}$ phases, or the non-tilted L_c-phase, form in single bilayer vesicles. These studies provided a direct link between liquid crystal physics and membrane physics and played a key role for the recognition of membrane research by the physicist. These early studies of defect formation in membranes have been reviewed in (163). Below we briefly mention some pertinent examples.

One example is that of the line defects separating fluid and gel like domains. These defects provide pathways for rapid lateral diffusion of membrane solutes, (analogous to "short circuit" diffusion in solid state physics (163–165). Another example is that of the chain packing defects around conically shaped integral proteins such as the voltage dependent Na^+-channels (166). These defects provide "cavities" – attracting small solutes such as local anesthetics which can fill the voids and impede the conductivity, (see Fig.12). This function of defects as attractive centers is reminiscent of the Cottrell Clouds of solutes formed around dislocations in solids which play a key role in the conditioning of material properties of metal alloys.

Density fluctuations in the lipid matrix ($\delta\rho$) may play a key role in enzyme activity and the conductivity of ion channels (166) which are particularly pronounced in liquid-solid domain boundaries, or around SPHM-rich domains, Fig. 6. The lateral density fluctuations may induce correlated changes in the cross-sectional area (ΔA) of the embedded proteins. In the case of ion channels for instance the changes in Na^+ conductivity were shown to obey an Arrhenius type behavior, $k = k_0 \exp\{-K\Delta A / k_B T\}$, where K is the membrane compression modulus and ΔA is the area difference of the hydrophobic domain of the ion channel in the non-conducting and the conducting state. The area compression modulus is inversely proportional to the density fluctuations, $\langle \delta\rho^2 \rangle / \rho^2 = K^{-1} \rho k_B T$, which increases (hence K decreases) drastically around the SPHM-rich domains and diverges at the boundaries of coexisting liquid-solid domains. In the case of sodium channels of the heart muscle $\Delta A \approx$ 0.04 nm^2. For densely packed lipid bilayers $K \approx 0.8\,\mathrm{Nm}^{-1}$ and hence $K\Delta A / k_B T \approx 8$. Defect

related local density fluctuations can thus drastically lower K, resulting in significantly higher ion conductivities

Another physiologically important role of membrane defects is illustrated in Fig. 12. Studies on model membranes indicate that lateral membrane inhomogeneities, such as those associated with asymmetrical protein inclusions or the boundaries between different lipid domains can largely acceleration of the exchange of specific lipids between outer leaflets of intracellular organelles (163). Pronounced defect-enhanced activities of this kind were reported for phospholipases, which appear to be most active at fluid-solid phase boundaries, Fluorescence microscopy studies showed that the enzyme is most active at the interface between solid and fluid domains (see (29, 167)).

Yet, another physiologically important effect of chain packing defects is the increase in the passive trans-membrane permeation of molecules and ions, which appears to increase with the square of the density fluctuations, $\left\langle \left| \delta\rho^2 \right| \right\rangle$. Recently, Heimburg et al suggested that the propagation of defects along the axon could control action potential propagation (168).

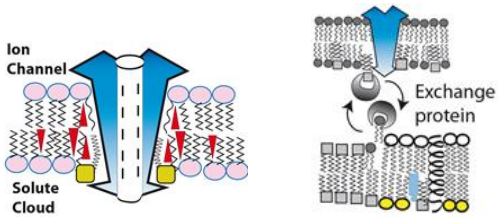

FIGURE 12 Left: Defect formation by local splay deformation of the lipid bilayer adjacent to conically shaped integral protein, such as Na^+-channels. The stress caused by the deformation can be relaxed when small lipophilic molecules such as local anesthetics migrate toward the defect, filling up the void thereby possibly impeding the ion conductivity, Right: Defects formed at lipid halos around integral proteins (top) or the rims of micro-domains (bottom) enhance the exchange of lipids between outer leaflets of membranes.

Lipid packing defects associated with membrane regions of high curvature can strongly affect enzyme activity in such regions as compared to planar membranes. The role of curvature in controlling enzymatic activity was first demonstrated by Paul Janmey and his coworkers who studied the generation of PI-3,4,5-P3 lipids by phosphoinositol-3-kinase (PI-3K), finding that vesicles with an average diameter of 100 nm are phosphorylated 100 times faster than vesicles with an average diameter greater than 300 nm (163). New interest in curvature-related membrane defects was boosted recently by studies concerning the binding of BAR-proteins to the necks connecting coated pits to the cell envelope. The neck formation is known to be controlled by BAR-proteins (such as endophilins (170)). Recent experimental studies provided evidence that the curvature induced packing defects resulting from the high curvature of the necks may account for the curvature sensing capacity of endophilin. The low lipid packing density in the defects enhances the binding of BAR proteins to the necks by facilitating the penetration of their amphipathic alpha helices (171). Finally we note that the role of defects as regulators of the dynamics of membrane processes is reminiscent of the role of defects for the plastic deformation of metals, suggesting analogies between the strategy of metallurgists to control the microstructure of metals and of nature to control the micro-anatomy of membranes.

8. BIOLOGICAL MEMBRANES AS ELASTIC SHELLS

8.1 MORPHOLOGY AND SHAPE TRANSITIONS OF SOFT ELASTIC SHELLS

The bending elasticity model of cell shape changes proposed by Helfrich (7) stimulated the interest of physicists and engineers working at the interface between physics and biology, resulting in the development of new concepts of soft shell elasticity. One example is the non-classical theory of scale dependent elastic properties of solid-like (tethered) membranes due to thermal excitations of long wavelength in-plane phonons and bending deformations (172). It stimulated the development of numerous new techniques enabling the measurement of the bending, shear and compression modulus elastic moduli, and the Young modulus (*E*) of cell envelopes. Great enthusiasm was raised by the discovery of undulation forces (173) and their role as regulators of cell adhesion, as discussed in Sec. 9.

Helfrich theory of membrane elasticity is a special case of the general Föppl-von Karman theory of shells. It was stimulated by Frank's theory of liquid crystal elasticity and led to relating membrane curvature deformations to the splay deformation of smectic liquid crystals. The membrane bending energy ΔG_{el} was expressed in terms of the principal curvatures, $1/R_1$ and $1/R_2$, of the bilayer's neutral plane, with the inside-out asymmetry of the bilayer accounted for by its mean spontaneous curvature C_0,

$$\Delta G_{el} = \frac{1}{2}\kappa \oiint dO(2H - C_0)^2 + \bar{\kappa} \oiint dOH_G \qquad (5)$$

Here $H = (1/R_1 + 1/R_2)/2$ and $H_G = 1/R_1R_2$ are the mean and Gaussian curvatures, respectively. κ and $\bar{\kappa}$ correspond to the splay, and saddle-splay elastic moduli introduced in liquid crystal physics (174). The integration extends over the membrane surface. Based on this equation, vesicle shapes and phase diagrams have been derived using two generic parameters: the spontaneous curvature, C_0, and the ratio A/V between the vesicle area to its volume, as discussed in detail by Seifert and Lipowsky (175).

One major success of the Helfrich homogeneous shell model was the prediction of some shape changes of erythrocytes, such as the discocyte to stomatocyte transition (see Fig. 13a). Direct experimental evidence for the application of the model to red blood cells was provided by the observation that this transition can be mimicked by single lipid component vesicles through temperature variations of the area-to-volume ratio (see (176) and Fig. 13b). Another success of the Helfrich model was the interpretation of conformational transitions of toroidal vesicles, (originally discovered by Bensimon and coworkers (177), see also (178)) resulting from the interplay between the mean (*H*) and Gaussian curvatures (H_G) (179); see Fig. 13c. It was shown that shapes of toroidal topology may involve one or several holes, and that for a given number of holes (called the genus of toroidal shapes) transitions between different shapes can occur without changing the bending energy (175, 180). A third success was the interpretation of the tension induced pearling instability of membrane tubes in terms of the Rayleigh instability (180).

The homogeneous shell model could not explain shape changes of vesicles formed from long chain lipids, which showed mainly spontaneous budding and formation of branched

tubules but no discocyte to stomatocyte transition. Svetina and Zeks showed that this shortcoming of the simple Helfrich model is remedied upon accounting for the coupling between the two monolayers of the shells (181). In fact, the important role of the coupling between the monolayers model had already been recognized by Evans in 1972 (182) but was ignored by the membrane community for several years. The theory of Evans accounted for the asymmetry of the membrane by assuming that the shape transitions of vesicles are determined by the initial difference ΔA_0 of the areas occupied by the inner (A_i) and outer monolayer (A_o).

Bilayer coupling has important consequences. If vesicles are prepared by swelling of bilayers in water the areas per lipid is roughly the same in the inner and the outer monolayer. Therefore the inner monolayer has to be compressed to form a closed shell. Since the exchange of lipids between the two monolayers is very slow (of the order of 12 hours for long chain lipids such as DPPC or DOPC). Freshly formed vesicles are initially not in mechanical equilibrium. Consequently, vesicles of long chain lipids exhibit only inside budding upon increasing the area to volume ratio (183).

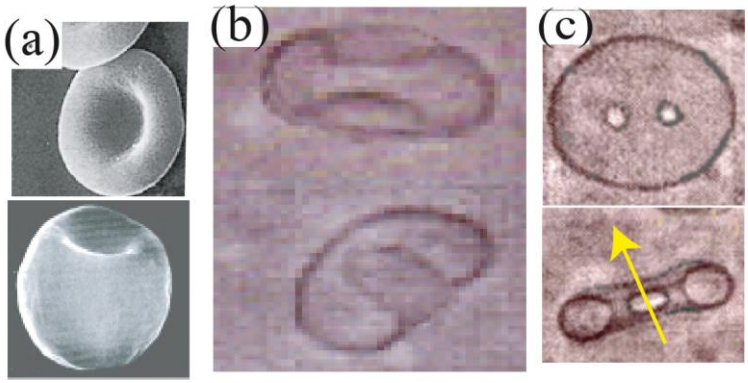

FIGURE 13 Experimental evidence for the simple Helfrich model of erythrocyte shape changes. **(a)** Discocyte to stomatocyte transition of red blood cells. **(b)** Discocyte to stomatocyte shape transition of vesicles of DMPC triggered by increasing the area to volume ratio *A/V*, achieved by increasing the temperature from 41°C to 42 °C.
(c) Demonstration of the generation of toroidal vesicles (image reproduced from (29)).

In 1997 a generalized elastic model accounting for the pre-stress generated by the tight coupling of the monolayers and the hindered flip flop was developed. The concept of spontaneous curvature was extended by introducing an effective spontaneous curvature consisting of two contributions, namely C_o (called local spontaneous curvature) and a term accounting for the intrinsic area difference $\Delta A_0/A_0$. The spontaneous curvature model and the area difference model were unified into the area difference elasticity (ADE) model, which interpolates between the two models. The ADE model has been extensively reviewed elsewhere (175) and we therefore point out only some major predictions.

- All three models yield about the same qualitative shape diagrams but the models differ concerning the prediction of the order of the transitions and the existence of metastable phase lines.
- The prolate and oblate shapes are stable over a large range of excess areas which could explain the robustness of the discocyte shape of erythrocytes against changes in osmolarity.

- The phase boundaries between two regimes of vesicle shapes may be may be separated by a spinodal line (SP). Shape transitions, such as budding, may therefore be drastically delayed, a fact that should be considered in experimental studies of vesicle shape changes-

.

8.2 SHAPE TRANSITIONS OF STRATIFIED SOFT SHELLS: THE RED BLOOD CELL

The compelling beauty of the Canham-Helfrich-Evans-Svetina-Zeks model delayed the interest of physicists in biologically important aspects of cell membranes structuring, such as the control of cell shapes by the intimate coupling of the lipid-protein bilayer to the membrane-associated cytoskeleton or the calculation of asymmetric cell shapes (184). To overcome this shortcomings the homogeneous shell model was extended in two directions:

Asymmetric cell shapes could be mimicked by considering the coupling between membrane curvature elasticity and in-plane phase separation. This issue has been studied by Andelman and Leibler (112), who combined the elastic energy functional ΔG_{ela} of the bending elasticity model with the free energy expression of the classical Cahn-Hilliard-Langer theory (see also (29) for a more extensive discussion). A few years later, Godzs and Gompper showed by MC simulations that the disk like cisternae of the ER could be formed by mixtures of lipid components one preferring positive curvature and the other prefers negative curvature (185).

Shortcomings of Helfrich model for the calculation of non-symmetric cell shapes were clearly pointed out in the PhD work of Stokke (186). He argued that non-symmetric red cell shapes, such as echinocytes and elliptocytes (in Fig. 14) can formed by the coupling of bending and shear deformation. With the sear elastic modulus a new length scale $\Lambda = \sqrt{\kappa/\mu}$ is introduced. For typical values of the bending modulus ($\kappa = 5\times10^{-19}$ J) and the shear modulus ($\mu = 7\times10^{-6}$ J/m^2) one finds $\Lambda \approx 300$ nm.

A rigorous elasticity theory of cell envelopes of general shapes, based on principles of differential geometry, has been first developed by Mark Peterson (187, 188). The theory allowed for the first time to calculate changes of the contour of cells induced by external forces, such as those applied by high frequency electric fields (189) or by shear deformation fields generating tank treading motions (190).

A comprehensive elastic theory of erythrocyte shapes was developed 30 years after the pioneering Canham-Helfrich by Wortis and collaborators (191). These authors calculated cell shapes by minimizing the total energy functional comprising (i) the bending elasticity expression of the ADE model ΔG_{ADE} and (ii) the sum of the extensional deformation and shear deformation ΔG_{ext} of the cytoskeleton, so that $\Delta G_{tot} = \Delta G_{ADE} + \Delta G_{Cyt}$.

The elastic energy of the cytoskeleton is expressed in terms of the rubber elasticity model of Mooney (first introduced by Skalak and Evans (192) in the field of membrane physics

$$\Delta G_{cyt} = \frac{K}{2}\oiint do(1-\lambda_1\lambda_2)^2 + \frac{\mu}{2}\oiint dO\left(\frac{\lambda_1}{\lambda_2}+\frac{\lambda_2}{\lambda_1}-2\right) \qquad (6)$$

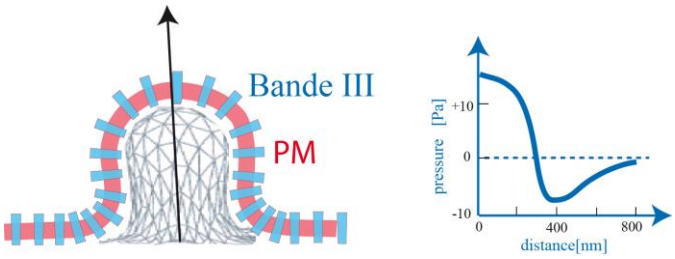

FIGURE 14 Variation of surface pressure of the lipid protein bilayer of red blood cell in the region of the cell surface forming a spicule. The network is stretched at the tip of the spicule and pulls at the membrane towards the inside. It is compressed at the base and exerts a pressure directed towards the outside. Note that the deformation of the cytoskeleton is associated with the redistribution of the membrane proteins, such as band III.

In conclusion, the Wortis model predicts that the shape changes of erythrocyte during their passage through blood vessels requires the ongoing reorganization of the spectrin-actin network. Concomitantly the membrane proteins Band III and glycophorin are expected to be constantly redistributed during the cell transport through the blood vessels which is an ATP consuming process.

8.3 MEMBRANE BENDING EXCITATIONS AND THEIR PHYSIOLOGICAL SIGNIFICANCE

The interest of many Soft Matter physicists in biomaterials was stimulated by the studies of cell membrane fluctuations by Brochard and Lennon (193) and Helfrich (173). In the former study it was shown that the long known flickering of erythrocytes was activated by bending excitations of the soft cell envelopes. Helfrich's work led to the beautiful picture of a membrane as a dynamically rough surface, which can regarded as being composed of cushions of dimension $\zeta_p \times \zeta_p$ performing independent Brownian motions in the normal direction to the membrane (194). Each collision of random local protrusions with adjacent surfaces was assumed to involve an energy of the order of k_BT, in analogy to molecules of an ideal gas hitting a solid wall. For tension free membranes at distance h from the wall the repulsive membrane pressure (which is equal to the transmitted energy per unit area) was shown to be given by (173, 194)

$$p_{disj} \approx k_BT / \zeta_p^2 h \propto (k_BT)^2 / \kappa h^3 \qquad (7)$$

Many functions of membrane undulation were discovered after Helfrich's publication. It became evident that the disjoining pressure plays a key role for the swelling of lipid multilayers and that it controls the adhesion of vesicles and cells compensates the Van der Waals attraction of lipid vesicles at distances $< h >\geq 20-30nm$. The tension induced freezing-in of the undulation was shown to triggered cell adhesion (195, 196). This effect was applied to measure the membrane bending modulus κ using the micropipette technique (197).

Further theoretical basis of the entropy driven interfacial forces was laid about eight years later by Lipowsky and Leibler (198). To account for the confinement of the membrane fluctuations they extended Helfrich's model by adding a harmonic interaction potential

$V(h) = V_0 + V''(h - h_0)^2 / 2$ that restricts these fluctuations. The total free energy functional can then be expressed as

$$\Delta G_{adh} = \iint dO \left\{ \frac{\kappa}{2} (\Delta u)^2 + \frac{\sigma}{2} \nabla u^2 + \frac{1}{2} \frac{\partial^2 V}{\partial x^2} \{h - h_o\}^2 \right\} \qquad (8)$$

This yields two observable length scales: the capillary length λ_c and the persistence length ζ_p given by

$$\lambda_c = \sqrt{\kappa / \sigma} \quad \text{and} \quad \zeta_p = \sqrt[4]{\kappa / V''} \qquad (9)$$

Here λ_c is a measure the maximum wavelength over which the membrane excitations are dominated by the bending excitations, and ζ_p accounts for the lateral extension of the membrane deformation induced by a local point force.

Experimental tests of the theories of membrane bending excitations became possible following the development of the Fourier spectroscopy of bending excitations of adhering giant vesicles and erythrocytes by reflection interference microscopy (RICM) combined with fast image processing (199). The spatial correlation function of the excitation amplitude $u(x,t)$, i.e.,

$$\langle u(x) u(x + \xi) \rangle = \zeta_\perp \exp\{-(x - x)^2 / \zeta_p^2\} \qquad (10)$$

and hence ζ_p could then be directly measured. By simultaneous measurement of the bending modulus ζ_p the force constant V'' of the interfacial potential could also be determined.

In 1987 Millner and Safran published a rigorous theory of shape fluctuations of vesicles by accounting for the boundary condition of constant volume in terms of the membrane tension γ (200). Their model paved the way for high precision measurement of membrane bending moduli by Fourier analysis of the contour of giant vesicles (183) with 0.5 μm wavelength resolution. The high precision method allowed to determine the number of shells of giant vesicles or the modification of κ by small concentrations of solutes and cholesterol.

8.4 RED BLOOD CELL MEMBRANES AS ACTIVELY DRIVEN SEMIFLEXIBLE STATISTICAL SURFACES

A surprising finding of the high precision RICM measurements of bending moduli of erythrocyte membranes was their astonishingly small bending modulus: $\kappa \approx 7 k_B T$ as compared to the value of $\kappa \approx 50 k_B T$ expected for the plasma membrane containing 50 mole% cholesterol (199, 201). Indeed, a parallel measurement of κ by Fourier analysis of the cell contour derived by phase contrast microscopy yielded a value of $50 k_B T$ (202), suggesting that the thermal excitation of the bending undulations are enforced by random chemical forces. These are expected to be caused by local fluctuations of lateral tension by the constituent coupling and un-coupling of the spectrin links from glycophorin which is associated with ATP turnover.

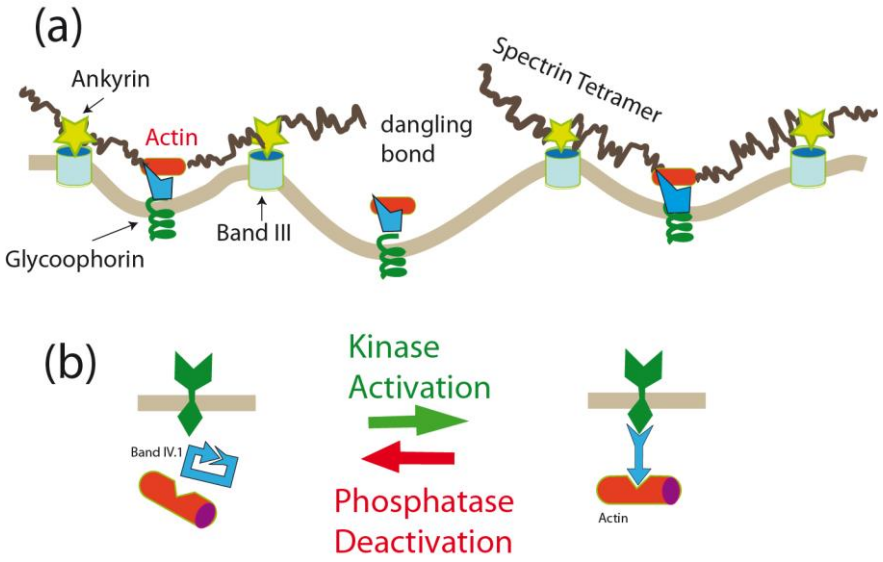

FIGURE 16 **(a)** Schematic view of composite cell envelope of erythrocytes with the lipid- protein bilayer exhibiting thermally and actively driven bending excitations. The undulatory excitations are limited by about 10% excess area of the bilayer with respect to the average area of the spectrin-actin network. They determine the distance between the two subshells and generate an excess membrane tension (194, 203). **(b)** The ongoing ATP.driven binding and unbinding of band IV.1 from glycophorin associated with the formation of dangling bonds enhances the bending amplitudes and could account for the non-thermal contributions to the undulations.

A sophisticated and rigorous two-shell model of the bending elasticity of stratified cell envelopes was developed by Safran and coworkers (203) allowing to evaluate the wavelength dependence of the mean square fluctuation amplitude in the membrane wavelength range $\Lambda \approx 0.5 - 2.5 \mu m$ measured by Zilker's Fourier spectroscopy (199). Korenstein and coworkers later provided direct evidence that the enhanced dynamic surface roughness is associated with ATP-turnover (204, 205), which provides some evidence for the model (201) of the enhancement of bending excitations by tension fluctuations proposed in Fig. 16.

It has been suggested that the over-excitation of the erythrocyte shell by fluctuating chemical forces can be described in terms of an effective temperature T_{eff} . $T_{eff} - T$ is measure of the excess undulation amplitude excited by stochastic chemical forces. It can be generally determined by simultaneously measuring the bending modulus by flicker analysis and other micromechanical techniques. Another method is based on the measurement of excess membrane tension by the micropipette technique (197). This approach has been adopted by Bassereau and coworkers to demonstrate the enhancement of bending membrane excitation by active chemical noise generated by ion translocation through membranes. Studying giant vesicles doped with reconstituted bacteriorhodopsin it was shown that light-driven proton pumping activity amplifies the bending undulation drastically (206). The chemical noise generated by proton influx can give rise to higher excess temperatures .

The following discussion of the physiological role of membrane flickering shows that more detailed studies of active excitation of flickering are expected to provide valuable insights into dynamic control of membrane processes.

8.5 THE PHYSIOLOGICAL ROLE OF MEMBRANE FLICKERING

In addition to erythrocytes, membrane bending undulations have been observed in various other cells, including endothelial cells and macrophages. These cells show mainly short wavelength excitations of $\Lambda \leq 1\mu m$ with ~10 nm root mean square amplitudes (207). This is remarkable, considering the fact that the bending and shear moduli of these composite shells are much larger ($\kappa \approx 1000\ k_B T$ and $\mu \approx 4 \times 10^{-4}\,\mathrm{Jm}^{-2}$) than those of erythrocytes. A challenging question is therefore whether membrane bending excitations may serve some purposes. Some possible answers are outlined below.

First and most importantly, the bending excitations prevent the non-specific adhesion of erythrocytes and macrophages to solid surfaces (see (207)) and the wall of the blood vessels. Second, erythrocytes do not possess intracellular transport mechanisms and the hydrodynamic flow induced by flickering in the cytoplasm (see (193)) could accelerate the exchange of hemoglobin between the rim of the cell and its center. Third, the disjoining pressure between the lipid-protein bilayer and the actin cytoskelton controls the distance between the two subshells of cell envelopes (203) and may inhibit the sticking of the actin cortex to the membrane. Fourth, the thermal excitations generate attractive isotropic forces between neighboring membrane-cytoskeleton linkers which is balanced by the tension of the entropic springs of the spectrin tetramers. This may serve the isotropic distribution of the spectrin-membrane linkers glycophorin and Band III and the dynamic softening of the cell envelope, as suggested by the stiffening of elliptocytes.

8.6 MOLECULAR ASPECTS OF MEMBRANE ELASTICITY

In parallel to the continuum theories of membrane elasticity, cell shape changes, undulations forces, and the various elegant experimental methods developed to measure elastic membrane moduli, many molecular-level models and theories have been proposed to calculate those moduli. These molecular-level model models range between simple pictures to rather elaborate theories employing realistic chain models and/or sophisticated electrostatic analyses. A simple yet very useful criterion for assessing the spontaneous curvature corresponding to a given lipid molecule is provided by the "packing parameter" $p = al / v$, where a, v, and l are the optimal area per lipid head group, the volume of the tail and its length (65); large p favoring positive curvature, whereas small p, as in the case with PE for instance, favors negative curvature, as observed the inverse hexagonal (H_{II}) phase. Phenomenological "compression models" have yielded insightful scaling relationships relating the bending rigidity to the lipid chain length and area per head group; see e.g., (63, 208, 209) and references therein. More sophisticated theories have also been proposed, taking into account the conformational (e.g., the rotational isomeric) statistics of the hydrocarbon lipid chains, and/or the electrostatic and excluded volume interactions between the head-groups. Any theory or computer simulation that yields information regarding the lateral pressure profile described in Fig. 4, can be used to calculate the elastic moduli using general relationships, such a

$$\kappa C_0 = \int z\pi(z)dz \quad , \quad \bar{\kappa} = -\int z^2\pi(z)dz \qquad (11)$$

Using the lateral pressure profile derived from E. (1) these elastic moduli, as well as an explicit expression for κ were derived, enabling to calculate the bending rigidities of single- and multi-component membranes (209, 210), showing very good qualitative and quantitative agreement with experiment. Over the years additional molecular-level theories and lattice models of membrane elasticity have been proposed, yet in recent years – in the spirit of time – most of the effort is invested on developing and applying large scale molecular-dynamics computer simulations.

9. CELL ADHESION: A MEMBRANE BASED PROCESS

Among the first questions that motivated the interest of physicists in cell adhesion was whether inter-membrane adhesion can be understood in terms of the classical DLVO theory of interfacial forces between charged surfaces. Studies of this question by Israelachvili and coworkers using the surface force apparatus (SFA) (65) and by Parsegian and coworkers using their osmotic stress technique (211) resulted in the first measurements of the Hamaker constants that measure the strength of the interaction between lipid bilayers and between membranes and solid surfaces (65). A second approach, pioneered by Bell and coworkers (212, 213), attempted to explain cell-to-cell adhesion in terms of the competition between specific attractive forces involving ("lock and key") adhesion receptors, and generic repulsion forces mediated by the glycoproteins forming the glycocalix. Analyzing the adhesion induced deformations of adhering cell envelopes they concluded that cells can be regarded as liquid droplets whose adhesion strength is determined by the Young-Laplace equation. This pioneering and fundamental study pointed out analogies between the adhesion of cells and partial wetting of solids by fluid droplets.

Below we briefly comment on two complementary points of view of membrane adhesion: (i) In Sec. 9.2 we outline the physicists' approach, emphasizing the mechanical aspects of cell adhesion and the interplay between membrane curvature elasticity, surface tension and the role of "linker" and "repeller" molecules. (ii) In Sec. 9.1 we briefly comment on the cell biologists' point of view where much emphasis is given to the molecular details and mutual interactions of the adhesive receptors.

9.1 MOLECULAR ASPECTS

Early biological studies were largely concerned with embryogenesis and tissue development, with particular emphasis on Cadherin mediated cell-cell adhesion. Takeichi (214), Steinberg (215, 216) and others (see e.g., (217) and references therein) have demonstrated that cadherin-mediated adhesion is strongly homophilic. Two early examples of this important aspect of cell adhesion are demonstrated in Fig. 17. The classical experiment of Towns and Holtfreter, was actually carried out before the role of adhesive receptors such as Cadherins for instance has been realized. The homophilic nature of receptor mediated adhesion was cast in simple physico-chemical terms by Steinberg and coworkers, an approach known as the Differential Adhesion Hypothesis (DAH), (215, 216). The DAH asserts that cell mixtures behave analogously to liquid mixtures of barely miscible molecules. Thus for

example, cells expressing epithelial (E) Cadherins, prefer adhering to cell cells expressing E-cadherins, rather than to, say, cells expressing neural (N) cadherins. Underlying this behavior is the fact that although the interaction between E-cadherin and N-Cadherin receptors is attractive, its strength (w_{NE}) is smaller than the average strength of the homophilic attractions (i.e., $w_{NE} < (w_{NN} + w_{NE})/2$). The differences between the attractive energies of the different kinds of receptors are small (typically just a few $k_B T$), yet since each cell is covered typically by tens to hundreds of thousands of molecules, the adhesive affinities between like cells are far stronger than those between unlike cells. Consequently, a mixture of cells expressing E and N cadherins strongly prefer to "phase segregate", resembling the behavior of a liquid mixture of immiscible molecules. This has been verified in various in-vivo systems and in-vitro assays, as illustrated in Fig.17 (214, 216, 217).

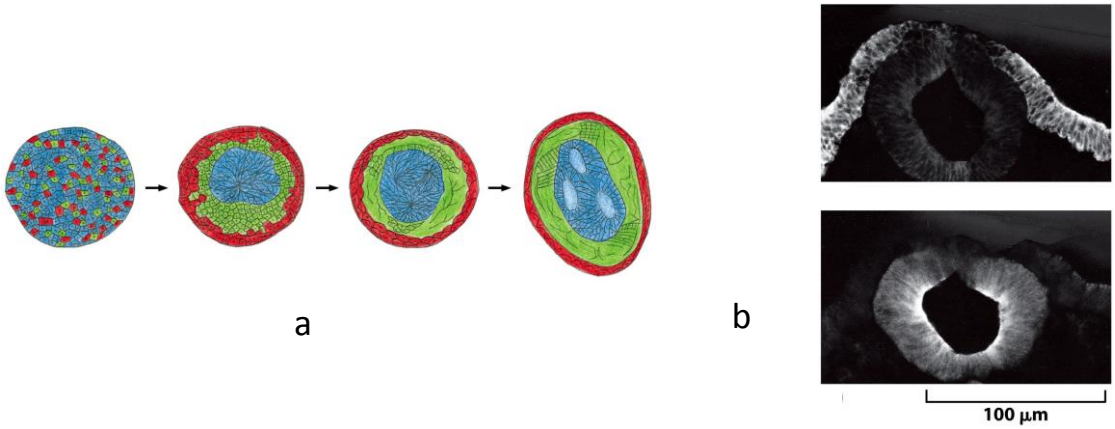

FIGURE 17 Experimental evidence for the homophilic nature of cadherin-mediated inter-cell adhesion. **(a)** In vitro self-organization of a cell mixture into an embryo-like structure. Following the dissociation (by alkali) of a piece of embryonic (amphibian neurola) tissue the cells were allowed to re-assemble. Initially, the cells re-assemble to form a uniformly mixed globule. After a while, due to the homophilic nature of the adhesion, segregation takes place, with neural cells (blue) constituting the inner core, mesodermal(green) in the middle layer and epithelial cells (red) in the outer shell. [A colored version of the figure adapted from the original landmark paper of Towns and Holtfreter (218)**.** **(b)** Cadherin segregation during the early stages of embryo morphogenesis. N-cadherins are expressed in the neural tube developing from the epithelial tissue where cells are held together by trans binding of E-cadherins (214).

Additional physical insights into the liquid droplet concept and quantitative information on the cohesive forces between cells were gained by Brochard and coworkers (219) by studying spherical cell assemblies by the micropipette aspiration technique. They showed that the cohesive force between spherical cell clusters increases monotonically with the cadherin expression. Studies of the dynamics of spreading of cells on surfaces showed some interesting analogies with the spreading viscoplastic fluid droplets.

While confirming the homophilicity of cell adhesion via selective (lock and key) forces among cell surface receptors, the adhesive energies associated with these forces do not explain the magnitude of cell-cell or cell-surface energies, as they do not account for the very important role played by the coupling of the adhesive receptors to the cytoskeleton, nor for

the important effects due to membrane curvature fluctuations. In other words, these assays provide little insight into the role of the composite cell membrane, or into the formation of focal adhesion complexes generally formed at the cell-cell and cell-tissue interface.

9.1 PHYSICAL BASIS

Important theoretical steps towards understanding the physical basis underlying the control of cell adhesion by soft elastic cell envelopes was made by Lipowsky and Seifert (220), Bruinsma (221) and Evans (222). These authors showed that the adhesion strength of fluid membranes can be quantified in terms of the spreading pressure W (the free energy of adhesion per unit area) given by the following equations:

$$W = \sigma(1-\cos\theta_c) \quad , \quad W = \frac{\kappa}{2}\left(\frac{1}{R_c}\right)^2 \qquad (1\ 2)$$

where σ is the membrane tension, κ is the bending modulus introduces in Eq. 5, θ_c is the contact angle and R_c is the radius of curvature of the shell at the contact line L_c (defined in Fig. 18). The first equation on the left side is the classical Young equation of capillary forces. The second equation accounts for the elastic energy associated with the bending of the membrane at the transition from the adhering to the free membrane area. The contact angle θ_c and the contact curvature R_c can be measured with high precision by using interferometric techniques, such as reflection interference contrast microscopy (RICM) (196, 221).

Experimental physics of cell adhesion research was boosted by development of planar solid supported membranes or patterned polymer films as models of cell and soft tissue surfaces. (reviewed until 2005 in (17)). This design opened up the possibility of reconstructing the contour of adhering soft shells, such as vesicles cells) with nm spatial resolution by the RICM technique enabling high precision measurements of the geometric parameters R_c and θ_c and hence of the free energies of adhesion (W in Eq. 5).

Simple model systems were designed to gain quantitative insight into the control of the state of adhesion by interplay of short range attraction forces mediated by specific linker pairs, long range repulsion forces mediated by glycoproteins and undulation forces and the adhesion induced membrane deformation. Giant vesicles doped with ligands of tissue (such as fibronectin or the antigenic oligosaccharide Sialyl Lewis X) served as test cells. Supported membranes exposing a conjugate CAM (such as integrin and selectins) mimicked the tissue or cell surface. To account for the repulsion forces mediated by the glycoproteins lipids exposing hydrophilic macromolecular head groups were added to one of the membranes. Unbinding forces between the linker pairs were measured by magnetic tweezer force microscopy. The state of the art of model membrane studies was reviewed recently (178). We therefore summarize below some important lessons learned from these model membrane studies

- An inevitable consequence of the balance of interfacial forces and elastic stresses summarized above is the decay of the adhesion zone into micro-domains of tight adhesion (formed by clusters of bound pairs of linkers) which are separated by non-adhering zones.
- Cell adhesion is a two-step process. The first step consists in the formation of clusters of linker pairs by the mechanism described above. In a secondary step, these clusters are stabilized by coupling of actin gel patches to the cytoplasmic tails of the CAMs.

In the case of integrin this coupling is mediated by the integrin-actin linkers talin and ezrin (illustrated in Fig. 13) which results in a drastic enhancement of the affinity of integrins for ligands (such as ICAM-I). This step plays a key role for the onset of lymphocyte transgression through the endothelial cell layers (see (223, 224)). In the case of cadherin-mediated cell-cell adhesion clusters of the linkers are stabilized by binding of their cytoplasmic tails to actin by β- and α-catenin. An important consequence of this linkage is a drastic increase of the membrane bending modulus and thus – according to Eq. 12 – of the binding strength *W*.

- A most surprising but important result is that values of the adhesion energy measured by contour a $W = 10^{-5} - 10^{-6}\,\mathrm{J\,m^{-2}}$ are several orders of magnitude smaller than the data estimated from the known density and binding energy of the linker pairs yielding $W \approx 10^{-3}\,\mathrm{J\,m^{-2}}$, (225). It was shown that reduction of W is a consequence of the two dimensional osmotic pressure exerted by the CAMs and repellers expelled from the adhesion domain. A rigorous theory of the initial process of adhesion domain formation by interplay of elastic and entropic forces was developed by Seifert and Smith (224).

Taken together the biomimetic studies show that the repulsive force mediated by the glycoproteins of the cell surface plays a key role for the softening of the adhesion strength and the rapid formation and dismantling of adhesion domains. It should be noted however, that many of the glycoproteins (such as Syndcans and CD44) can act as cell adhesion molecules which mediate the adhesion of stroma cells to macromolecules of the extracellular matrix, such as collagen networks. Most cell adhesion molecules expose cytoplasmic domains which mediate their coupling to the actin cortex through specific linkers, such as talin and ezrin. The global distribution of the linkers can be controlled by the actin- microtubule crosstalk which plays a key role for the global polarization of cells. Several physiologically relevant examples of the control of cell adhesion by microtubule-actin crosstalk have been recently reviewed in (178) and the interested reader is referred to this paper.

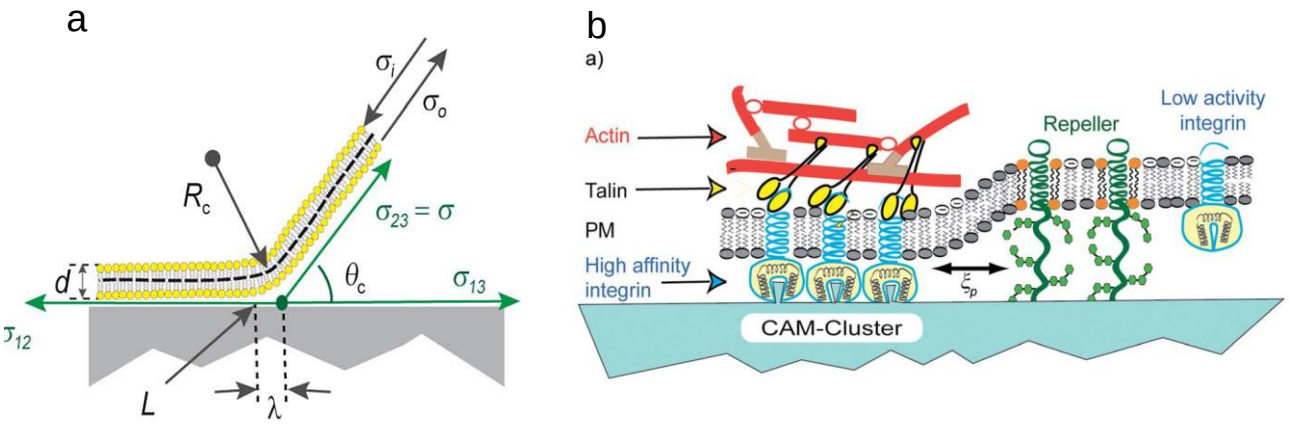

FIGURE 18 **(a)** Mechanical equilibrium of the interfacial tension and the bending moment at the contact line L_c of the adhesion zone. The surface tensions σ_{ij} are measures of the interfacial energies. R_c is the radius of membrane curvature at the contact line L_c. (see also (220)) **(b)** Decay of the cell

substrate interface into domains of tight adhesion (formed by integrin clustering) and weakly adhering zones which are separated from the substrate by long range forces mediated by glycoproteins of the glycocalix and undulation forces. The binding strength of the initially formed clusters of integrin is enforced first, by the drastic increase of the affinity of the CAMs for ligands of the tissue (such as fibronectin) and secondly, by the increase of the membrane bending stiffness induced by coupling of actin gel patches to the cytoplasmic domains of integrin (following Eq. 12). The width of the transition zone between the two states of adhesion is equal to the persistence length ζ_p appearing in Eq. 7. (Images adopted from (178)).

9.3 AN OUTLOOK

The design of sophisticated model systems of cell adhesion together with the development of new experimental techniques and thermomechanical theories have provided new insight into the control of cell adhesion by intermolecular forces and elastic stresses (178). It is certainly a long way to design model systems which can mimic the active control of cell adhesion mediated by coupling of CAM-clusters to the actin cortex. At present, a more promising strategy is to apply the methods and concepts developed over the last 40 years to study the adhesion of living cells on bio-functionalized surfaces. The bending moduli, the membrane tensions and the adhesion strengths can be measured by applying lift forces and hydrodynamic shear forces (213, 226). Insights into the control of the adhesion strength mediated by coupling of the actin cortex to the intracellular domains of the CAM-clusters can be gained by mutations of the proteins regulating actin membrane coupling, such as talin, see e.g., (226).

The combined study of *in vitro* systems and natural cells has shed new light on the long standing question, how myelin sheath form tightly packed multilayers of collapsed cell lobes around axons. The first insights were provided by Janshoff and coworkers who measuremed the forces between the inner leaflets of the plasma membranes mediated by the electrostatic interaction of the myelin basic protein (227). Recent experiments solved another part of the enigma by showing that membrane lobes protruding from oligodentrocytes cells (forming myelin sheets in the brain) adhere strongly to axon surface after down-regulation of the genetic expression of both the repellent glycoproteins and the glycolipids (228). The inter-membrane distance of 2nm is determined by the van der Waals attraction which is balanced by the repulsion mediated by an non-charged integral protein.

10. A SHORT OUTLOOK: WHERE WE STAND AND WHERE TO GO

In the last 40 years our understanding of the physical basis of the self-organisation of biological membrane has advanced dramatically, owing to the comparative study of model systems and biological membranes. This breakthrough was made possible by the interactive development of new physical techniques and novel theoretical concepts and computational tools. There are still many unsolved problems. Many of these are due to our difficulties to deal with the thermo-mechanics of multicomponent systems under non-equilibrium conditions.

It appears that there are two directions to go. One strategy is to mimic the structure and function of real composite membranes by reconstitution of active actin and microtubule

networks into giant vesicles with reconstituted ion channels and cell adhesion molecules. Such artificial cell organelles are also of growing interest as smart drug delivery systems.

An easier strategy may be to study natural membranes and their structural and functional modifications by specific mutations or signalling molecules. This requires that physicists realize that the biological membranes are composite shells and that their molecular architecture is constantly remodelled by biochemical processes to adapt the cell structure and function to the cells physiological needs.

Studies of natural membrane processes teaches us how to regulate the structure and physical properties of complex materials by local changes of the chemical composition. A future benefit of such painstaking studies may be that we learn how to design smart materials with the capacity to adapt their physical properties to environmental conditions.

LIST OF ABBREVIATIONS

ADE model: Area difference elasticity model; BLM: black; DLVO theory: Derjaguin-Landau-Verwey-Overbeek theory of the stability of colloidal suspensions; EISF: elastic incoherent scattering factor. FCS: fluorescence correlation spectroscopy; FTIR: Fourier transform infrared spectroscopy; MARCKS: Myristoylated Alalnine-Rich C-Kinase Substrate; PLC-Cγ : Phospholipase-Cγ (an enzyme generating inositol 1,4,5-trisphosphate and diacylglycerol (DAG) from PI-4,5-P2); PI-3K: Phosphoinositid-3-kinase (generator of PI-3,4,5-P3); RICM: reflection interference contrast microscopy (also called Interference Reflection Microscopy (IRM). SFA: surface force apparatus.

Lipid abbreviations and nomenclature: The structure of each type of lipid is characterized by the structure of the head groups and the number of C-atoms (n) and double bonds (m) of the hydrocarbon chains.
Types of lipids: PC: phosphatidylcholine; PE: phosphatidylethanolamine;
PS: phosphatidylserine; PI: phosphoinositides (including PI-4,5-P2 and PI-3,4,5-P3, also abbreviated as PtdIns(4,5)P2 and PtdIns (3,4,5)P3); DAG: diacylglycerol (DAG)
Examles: PC: C16:0;C16:0 and PC: C16:0, C18;1 stand for dipalmitoylphosphatidylcholin and palmitol-strearoyl phosphatidylcholine, respectively.

ACKNOWLEDGEMENTS

E.S. grateful acknowledges financial support by the Excellence Initiative of the Technical University Munich and The Center for NanoScience (CeNS) at the Ludwig- Maximilian-University (LMU) Munich. ABS thanks the support of the Fritz Haber Research Center supported by the Minerva Foundation.

BIBLIOGRAPHY

1. Gorter, E., and F. Grendel. 1925. ON BIMOLECULAR LAYERS OF LIPOIDS ON THE CHROMOCYTES OF THE BLOOD. J. Exp. Med. 41: 439–43.
2. Danielli, J.F., and H. Davson. 1935. A contribution to the theory of permeability of thin films. J. Cell. Comp. Physiol. 5: 495–508.
3. Singer, S.J., and G.L. Nicolson. 1972. The fluid mosaic model of the structure of cell membranes. Science (80-.). 175: 720–731.
4. Sackmann, E. 1983. Physical Foundation of the Molecular Organization and Dynamics of Membranes in Biophysics. In: Biophysics. Berlin: Springer Verlag.
5. Luzzati, V. 1968. X-ray duffraction studies of lipid-water systems. In: Chapman D, editor. Biological Membranes, Vol. 1. London: . pp. 71–123.
6. Luzzati, V., and a Tardieu. 1974. Lipid Phases: Structure and Structural Transitions. Annu. Rev. Phys. Chem. 25: 79–94.
7. Helfrich, W. 1973. Elastic properties of lipid bilayers: theory and possible experiments. Z. Naturforsch. 28: 693–703.
8. Bessis, M. 1973. Living Blood Cells and their UltrastructueNo Title. Berlin-Heidelberg-New York: Apringer Verlag.
9. Shen, B.W., R. Josephs, and T.L. Steck. 1986. Ultrastructure of the intact skeleton of the human erythrocyte membrane. J. Cell Biol. 102: 997–1006.
10. Legendre, K., S. Safieddine, P. Küssel-Andermann, C. Petit, and A. El-Amraoui. 2008. alphaII-betaV spectrin bridges the plasma membrane and cortical lattice in the lateral wall of the auditory outer hair cells. J. Cell Sci. 121: 3347–3356.
11. Hladky, S.B., and D. a Haydon. 1972. Ion transfer across lipid membranes in the presence of gramicidin A. I. Studies of the unit conductance channel. Biochim. Biophys. Acta. 274: 294–312.
12. Bamberg, E., and P. Läuger. 1973. Channel formation kinetics of gramicidin A in lipid bilayer membranes. J Membr Biol. 11: 177–194.
13. Kolb, H.-A., and G. Boheim. 1978. Analysis of the multi-pore system of alamethicin in a lipid membrane. J. Membr. Biol. 38: 151–191.
14. Conti, F., Wanke, E. 1975. Channel noise in nerve membranes and lipid bilayers. Q. Rev. Biophys. 8: 451–506.
15. Chernomordik, L., A. Chanturiya, J. Green, and J. Zimmerberg. 1995. The hemifusion intermediate and its conversion to complete fusion: Regualtion by membrane composition. Biophys. J. 69: 922–929.
16. Li, F., F. Pincet, E. Perez, C.G. Giraudo, D. Tareste, and J.E. Rothman. 2011. Complexin activates and clamps SNAREpins by a common mechanism involving an intermediate energetic state. Nat. Struct. Mol. Biol. 18: 941–946.
17. Tanaka, M., and E. Sackmann. 2005. Polymer-supported membranes as models of the cell surface. Nature. 437: 656–663.
18. Seddon, J.M., and R.H. Templer. 1995. Polymorphism of lipid-water systems. In: Lipowsky R, E Sackmann, editors. Structure and Dynamics of Membranes. Amsterdam: Elsevier. pp. 98–160.
19. Voeltz, G.K., W.A. Prinz, Y. Shibata, J.M. Rist, and T.A. Rapoport. 2006. A Class of Membrane Proteins Shaping the Tubular Endoplasmic Reticulum. Cell. 124: 573–586.
20. Sackmann, E. 2014. Endoplasmatic reticulum shaping by generic mechanisms and protein-induced spontaneous curvature. Adv. Colloid Interface Sci. 208: 153–160.
21. Sackmann, E., H. Träuble, H.J. Galla, and P. Overath. 1973. Lateral diffusion, protein mobility, and phase transitions in Escherichia coli membranes. A spin label study. Biochemistry. 12: 5360–5369.
22. Seelig, J. 1977. Deuterium Magnetic-Resonance Theory and Applications to Lipid Membranes. Q. Rev. Biophys. 10: 353–418.
23. Mely, B., J. Charvolin, and P. Keller. 1975. OF THEIR LATERAL PACKING IN LYOTROPIC LIQUID CRYSTALS. 15: 161–173.
24. Mantsch, H.H., and R.N. McElhaney. 1991. Phospholipid phase transitions in model and biological

membranes as studied by infrared spectroscopy. Chem. Phys. Lipids. 57: 213–226.

25. Esmann, M., and D. Marsh. 1985. Spin-label studies on the origin of the specificity of lipid-protein interactions in Na+,K+-ATPase membranes from Squalus acanthias. Biochemistry. 24: 3572–3578.

26. König, B.W., S. Krueger, W.J. Orts, C.F. Majkrzak, N.F. Berk, J. V Silverton, and K. Gawrisch. 1996. Neutron Reflectivity and Atomic Force Microscopy Studies of a Lipid Bilayer in Water Adsorbed to the Surface of a Silicon Single Crystal. Langmuir. 12: 1343–1350.

27. König, S., W. Pfeiffer, T. Bayerl, D. Richter, and E. Sackmann. 1992. Molecular dynamics of lipid bilayers studied by incoherent quasi-elastic neutron scattering. J. Phys. II. 2: 1589–1615.

28. Buldt, G., H.U. Gally, A. Seelig, and J. Seelig. 1978. Neutron diffraction studies on selectively deuterated phospholipid bilayers. Nature. 271: 182–184.

29. E. Sackmann. 1995. Physical basis of self-organization and function of membranes: physics of vesicles. In: R. Lipowsky, E. Sackmann, editors. Structure and Dynamics of Membranes. Amsterdam: Elsevier. pp. 213–304.

30. Overath, P., and H. Trauble. 1970. Phase Transitions in Cells, Membranes, and Lipids of Escherichia coli by Fluorescent Probes, Light Scattering and Dilatometry. Biochemistry. 12: 2625–2634.

31. McIntosh, T.J., and S.A. Simon. 1986. Area per molecule and distribution of water in fully hydrated dilauroylphosphatidylethanolamine bilayers. Biochemistry. 25: 4948–4952.

32. Wilkinson, D. a, and J.F. Nagle. 1981. Dilatometry and calorimetry of saturated phosphatidylethanolamine dispersions. Biochemistry. 20: 187–92.

33. Privalov, G., V. Kavina, E. Freire, and P.L. Privalov. 1995. Precise scanning calorimeter for studying thermal properties of biological macromolecules in dilute solution. Anal. Biochem. 232: 79–85.

34. Shimshick, E.J., and H.M. McConnell. 1973. Lateral phase separation in phospholipid membranes. Biochemistry. 12: 2351–2360.

35. Mouritsen, O.G. 1991. Theoretical models of phospholipid phase transitions. Chem. Phys. Lipids. 57: 179–194.

36. Mouritsen, O.G. 2005. Life–as a matter of fat: the emerging science of lipidomics. Heidelberg: Springer.

37. Silvius, D.R. Thermotropic Phase Transitions of Pure Lipids in Model Membranes and Their Modifications by Membrane Proteins. New York: John Wiley & Sons, Inc.1982.

38. Coolbear, K.P., C.B. Berde, and K.M. Keough. 1983. Gel to liquid-crystalline phase transitions of aqueous dispersions of polyunsaturated mixed-acid phosphatidylcholines. Biochemistry. 22: 1466–1473.

39. Nagle, J.F. 1973. Theory of biomembrane phase transitions. J. Chem. Phys. 58: 252.

40. Scott Jr., H.L. 1975. Some models for lipid bilayer and biomembrane phase transitions. J. Chem. Phys. 62: 1347–1353.

41. A. Caillé, D. Pink, F. De Verteuil, M.J.Z. 1980. Theoretical models for quasi-two-dimensional mesomorphic monolayers and membrane bilayers. Can. J. Physics, , 58(5) , 10.1139/p80-083. 58: 581–611.

42. Jähnig, F. 1981. Critical effects from lipid-protein interaction in membranes. I. Theoretical description. Biophys. J. 36: 329–345.

43. de Gennes, P.G. 1974. General features of lipid organization. Phys. Lett. A. 47: 123–124.

44. Schröder, H. 1977. Aggregation of proteins in membranes. An example of fluctuation-induced interactions in liquid crystals. J. Chem. Phys. 67: 1617–1619.

45. Marčelja, S. 1974. Chain Ordering in Liquid Crystals II. Structure of Bilayer Membranes. Biochim. Biophys. Acta. 367: 165–176.

46. Marčelja, S. 1976. Lipid-mediated protein interaction in membranes. Biochim. Biophys. Acta. 455: 1–7.

47. Cevc, G. 1991. Polymorphism of the bilayer membranes in the ordered phase and the molecular origin of the lipid pretransition and rippled lamellae. Biochim. Biophys. Acta - Biomembr. 1062: 59–69.

48. Nelson, D. 1987. Theory of the crumpling transition. In: Nelsonj, D, Piran, T and Weinberg S, editor. Statistical Mechanics of Surfaces and Membranes. World Scientific, Singapore. pp. 137–155.

49. Akabori, K., and J.F. Nagle. 2015. Structure of the DMPC lipid bilayer ripple phase. Soft Matter. 11: 918–926.

50. Albrecht, O, Gruler, H, Sackmann, E. 1978. Polymorphism of phospholipid monolayers. J. Phys. 39:

301–313.

51. McConnell, H.M., and V.T. Moy. 1988. Shapes of finite two-dimensional lipid domains. J. Phys. Chem. 92: 4520–4525.

52. McConnell, H.M. 1989. Theory of Hexagonal and Stripe Phases of Monolayers. PNAS. : 3452–3455.

53. Möhwald, H. 1995. Lipid Monolayers. In: Lipowsky, R and Sackmann E, editor. Handbook of Biological Physics Vol 1A,. Amsterdam: . pp. 161–211.

54. Seelig, J., and W. Niederberger. 1974. Two pictures of a lipid bilayer. A comparison between deuterium label and spin-label experiments. Biochemistry. 13: 1585–1588.

55. König, S., T.M. Bayerl, G. Coddens, D. Richter, and E. Sackmann. 1995. Hydration dependence of chain dynamics and local diffusion in L-alpha-dipalmitoylphosphtidylcholine multilayers studied by incoherent quasi-elastic neutron scattering. Biophys. J. 68: 1871–1880.

56. Wiener, M.C., and S.H. White. 1992. Structure of a fluid dioleoylphosphatidylcholine bilayer determined by joint refinement of x-ray and neutron diffraction data. III. Complete structure. Biophys. J. 61: 434–447.

57. Dill, K.A., and P.J. Flory. 1980. Interphases of chain molecules: Monolayers and lipid bilayer membranes. Proc. Natl. Acad. Sci. 77: 3115–3119.

58. Leermakers, F.A.M., and J.M.H.M. Scheutjens. 1988. Statistical thermodynamics of association colloids. III. The gel to liquid phase transition of lipid bilayer membranes. J. Chem. Phys. 89: 6912.

59. van der Ploeg, P. Berendsen, H.J.C., and P. van der Ploeg. 1982. Molecular dynamics simulation of a bilayer membrane. J. Chem. Phys. 76: 3271.

60. Jähnig, F. 1979. Molecular theory of lipid membrane order. J. Chem. Phys. 70: 3279.

61. Gruen, D.W.R. 1985. A model for the chains in amphiphilic aggregates. 1. Comparison with a molecular dynamics simulation of a bilayer. J. Phys. Chem. 89: 146–153.

62. Ben-Shaul, A., I. Szleifer, and W.M. Gelbart. 1985. Chain organization and thermodynamics in micelles and bilayers. I. Theory. J. Chem. Phys. 83: 3597–3611.

63. Ben-Shaul, A. 1995. Molecular theory of chain packing, elasticity and lipid protein interaction in lipid bilayers. In: Lipowsky R, E Sackmann, editors. Structure and Dynamics of Membranes. Amsterdam: Elsevier. pp. 359–402.

64. Israelachvili, J.N., J. Mitchell, and B.W. Ninham. 1976. Theory of self-assembly of hydrocarbon amphiphiles into micelles and bilayers. J.Chem.Soc.Farad.2. 72: 1525–1568.

65. Israelachvili, J.N. 2010. Intermolecular and Surface Forces. .

66. Seelig, J., and N. Waespe-Sarcevic. 1978. Molecular order in cis and trans unsaturated phospholipid bilayers. Biochemistry. 17: 3310–3315.

67. Heller, H., M. Schaefer, and K. Schulten. 1993. Molecular dynamics simulation of a bilayer of 200 lipids in the gel and in the liquid crystal phase. J. Phys. Chem. 97: 8343–8360.

68. Fattal, D.R., and A. Ben-shaul. 1994. Mean-field calculations of chain packing and conformational statistics in lipid bilayers: comparison with experiments and molecular dynamics studies. Biophys. J. 67: 983–995.

69. Op den Kamp, J. a, M.T. Kauerz, and L.L. van Deenen. 1975. Action of pancreatic phospholipase A2 on phosphatidylcholine bilayers in different physical states. Biochim. Biophys. Acta. 406: 169–177.

70. Seigneuret, M., and P.F. Devaux. 1984. ATP-dependent asymmetric distribution of spin-labeled phospholipids in the erythrocyte membrane: relation to shape changes. Proc. Natl. Acad. Sci. U. S. A. 81: 3751–3755.

71. Steck, T.L., and Y. Lange. 2010. Cell cholesterol homeostasis: Mediation by active cholesterol. Trends Cell Biol. 20: 680–687.

72. Zheng, G., B. Tian, F. Zhang, F. Tao, and W. Li. 2011. Plant adaptation to frequent alterations between high and low temperatures: remodelling of membrane lipids and maintenance of unsaturation levels. Plant. Cell Environ. 34: 1431–42.

73. Wu, S., and H. McConnell. 1975. Phase Separations in Phospholipid Membranes. Biochemistry. 14: 847–854.

74. Vist, M.R., and J.H. Davis. 1990. Phase equilibria of cholesterol/dipalmitoylphosphatidylcholine

mixtures: 2H nuclear magnetic resonance and differential scanning calorimetry. Biochemistry. 29: 451–464.

75. Mabrey, S., P.L. Mateo, and J.M. Sturtevant. 1978. High-sensitivity scanning calorimetric study of mixtures of cholesterol with dimyristoyl- and dipalmitoylphosphatidylcholines. Biochemistry. 17: 2464–2468.

76. Evans, E., and D. Needham. 1986. Giant vesicle bilayers composed of mixtures of lipids, cholesterol and polypeptides. Thermomechanical and (mutual) adherence properties. Faraday Discuss. Chem. Soc. : 267–280.

77. Knoll, W., G. Schmidt, and E. Sackmann. 1983. Critical demixing in fluid bilayers of phospholipid mixtures. A neutron diffraction study. J. Chem. Phys. 79: 3439–3442.

78. Knoll, W., G. Schmidt, K. Ibel, and E. Sackmann. 1985. Small-angle neutron scattering study of lateral phase separation in dimyristoylphosphatidylcholine-cholesterol mixed membranes. Biochemistry. 24: 5240–5246.

79. Komura, S., H. Shirotori, P.D. Olmsted, and D. Andelman. 2004. Lateral phase separation in mixtures of lipids and cholesterol systems. 321: 7.

80. Elliott, R., I. Szleifer, and M. Schick. 2006. Phase Diagram of a Ternary Mixture of Cholesterol and Saturated and Unsaturated Lipids Calculated from a Microscopic Model. Phys. Rev. Lett. 96: 098101.

81. Reinl, H., T. Brumm, and T.M. Bayerl. 1992. Changes of the physical properties of the liquid-ordered phase with temperature in binary mixtures of DPPC with cholesterol. Biophys. J. 61: 1025–1035.

82. Tu, K., M.L. Klein, and D.J. Tobias. 1998. Constant-pressure molecular dynamics investigation of cholesterol effects in dipalmitoylphosphatidylcholine bilayer. Biophys. J. 75: 2147–2156.

83. Brzustowicz, M.R., V. Cherezov, M. Caffrey, W. Stillwell, and S.R. Wassall. 2002. Molecular organization of cholesterol in polyunsaturated membranes: microdomain formation. Biophys. J. 82: 285–298.

84. Maulik, P.R., and G.G. Shipley. 1996. N-palmitoyl sphingomyelin bilayers: Structure and interactions with cholesterol and dipalmitoylphosphatidylcholine. Biochemistry. 35: 8025–8034.

85. Döbereiner, H.G., J. Käs, D. Noppl, I. Sprenger, and E. Sackmann. 1993. Budding and fission of vesicles. Biophys. J. 65: 1396–403.

86. Sackmann, E. 2006. Thermo-elasticity and adhesion as regulators of cell membrane architecture and function. J. Phys. Condens. Matter. 18: R785–R825.

87. Wimley, W.C., and S.H. White. 1996. Experimentally determined hydrophobicity scale for proteins at membrane interfaces. Nat. Struct. Biol. 3: 842–848.

88. Marsh, D. 1990. Lipid-protein interactions in membranes. FEBS Lett. 268: 371–375.

89. Mouritsen, O.G., and M. Bloom. 1984. Mattress model of lipid-protein interactions in membranes. Biophys. J. 46: 141–153.

90. Riegler, J., and H. Möhwald. 1986. Elastic interactions of photosynthetic reaction center proteins affecting phase transitions and protein distributions. Biophys. J. 49: 1111–1118.

91. Gruler, H. 2015. Chemoelastic effect of membranes. Z. Naturforsch. C. 30: 608–614.

92. Fattal, D.R., and A. Ben-Shaul. 1993. A molecular model for lipid protein interaction in membranes: The role of hydrophobic mismatch. Biophys. J. 65: 1795–1809.

93. Goulian, M., R. Bruinsma, and P. Pincus. 1993. Long-range forces in heterogeneous fluid membranes. Eur. Lett. 22: 145–150.

94. Aranda-Espinoza, H., A. Berman, N. Dan, P. Pincus, and S.A. Safran. 1996. Interaction between inclusions embedded in membranes. Biophys. J.J. 71: 648–656.

95. Killian, J.A. 1998. Hydrophobic mismatch between proteins and lipids in membranes. Biophys. Biochim. 1376: 401–416.

96. Siegel, D.P., and R.M. Epand. 1997. The Mechanism of Lamellar-to-Inverted Hexagonal Phase Transitions in Phosphatidylethanolamine: Implications for Membrane Fusion Mechanisms. Biophys. J. 73: 3089–3111.

97. May, S., and A. Ben-Shaul. 1999. Molecular theory of lipid-protein interaction and the Lalpha-HII transition. Biophys. J. 76: 751–767.

98. Ludtke, S.J., K. He, W.T. Heller, T.A. Harroun, L. Yang, and H.W. Huang. 1996. Membrane pores induced by magainin. Biochemistry. 35: 13723–13728.

99. Epand, R.M., Y. Shai, J.P. Segrest, and G.M. Anantharamaiah. 1995. Mechanisms for the modulation of membrane bilayer properties by amphiphatic helical peptides. Biopolym. (Peptide Sci. 37: 319–338.

100. Huang, H.W. 1986. Deformation free energy of bilayer membrane and its effect on gramicidin channel lifetime. Biophys. J. 50: 1061–1070.

101. Zemel, A., D.R. Fattal, and A. Ben-Shaul. 2003. Energetics and self-assembly of amphipathic peptide pores in lipid membranes. Biophys. J. 84: 2242–2255.

102. Zuckermann, M.J., and T. Heimburg. 2001. Insertion and pore formation driven by adsorption of proteins onto lipid bilayer membrane-water interfaces. Biophys. J. 81: 2458–2472.

103. Lin, J.-H., and A. Baumgaertner. 2000. Stability of a Melittin pore in a lipid bilayer: a molecular dynamics study. Biophys. J. 78: 1714–1724.

104. Helfrich, P., and E. Jakobsson. 1990. Calculation of deformation energies and conformations in lipid membranes containing gramicidin channels. Biophys. J. 57: 1075–1084.

105. Goulian, M., O.N. Mesquita, D.K. Fygenson, C. Nielsen, O.S. Andersen, and a Libchaber. 1998. Gramicidin channel kinetics under tension. Biophys. J. 74: 328–337.

106. Sens, P., and M.S. Turner. 2004. Theoretical model for the formation of caveolae and similar membrane invaginations. Biophys. J. 86: 2049–2057.

107. Bretscher, M.S., and S. Munro. 1993. Cholesterol and the Golgi Apparatus phe. Science (80-.). 261: 1280–1281.

108. Kurrle, A., P. Rieber, and E. Sackmann. 1990. Reconstitution of transferrin receptor in mixed lipid vesicles. An example of the role of elastic and electrostatic forces for protein/lipid assembly. Biochemistry. 29: 8274–8282.

109. Simons, K., and E. Ikonon. 1997. Functional rafts in cell membranes. Nature. 387: 569–572.

110. Schwartz, S.L., C. Cao, O. Pylypenko, A. Rak, and A. Wandinger-Ness. 2008. Rab GTPases at a glance. J. Cell Sci. 121: 246–246.

111. Baumgart, T., T.S. Hess, and W.W. Webb. 2003. Imaging coexisting fluid domains in biomembrane models coupling curvature and line tension. Nature. 425: 821–824.

112. Leibler, S., and D. Andelman. 2013. Ordered and curved meso-structures in membranes and amphiphilic films. 48: 2013–2018.

113. Träuble, H., and H. Eibl. 1974. Electrostatic effects on lipid phase transitions: membrane structure and ionic environment. Pnas. 71: 214–219.

114. Jähnig, F. 1976. Electrostatic free energy and shift of the phase transition for charged lipid membranes. Biophys. Chem. 4: 309–318.

115. Cevc, G. 1990. Membrane electrostatics. Biochim. Biophys. Acta. 1031: 311–382.

116. Andelman, D. 1995. Electrostatic properties of membranes: The Poisson-Boltzmann theory. In: Lipowsky R, E Sackmann, editors. Structure and Dynamics of Membranes. Amsterdam: Elsevier. pp. 603–642.

117. Markovich, T., D. Andelman, and R. Podgornik. 2016. Charged Membranes: Poisson-Boltzmann theory, DLVO paradigm and beyond. In: Safinya C, J Rädler, editors. Handbook of Lipid Membranes. .

118. Parsegian, V.A., and D. Gingell. 1972. On the electrostatic interaction across a salt solution between two bodies bearing unequal charges. Biophys. J. 12: 1192–1204.

119. Gerke, V., C.E. Creutz, and S.E. Moss. 2005. Annexins: linking Ca2+ signalling to membrane dynamics. Nat. Rev. Mol. Cell Biol. 6: 449–461.

120. Vogt, B., P. Ducarme, S. Schinzel, R. Brasseur, and B. Bechinger. 2000. The topology of lysine-containing amphipathic peptides in bilayers by circular dichroism, solid-state NMR, and molecular modeling. Biophys. J. 79: 2644–56.

121. Sackmann, E. Lecture note: Physics of Functional Microdomains. www.biophy.de. .

122. McLaughlin, S., and A. Aderem. 1995. The myristoyl-electrostatic switch: A modulator of reversible protein-membrane interactions. TIBS. 20: 272–276.

123. Murray, D., B. Honig, and S. McLaughlin. 1998. Sequestration of PIP2 into lateral domains formed by

basic peptides. FASEB J.l. 12: A1395–A1395.

124. Wang, J.Y., A. Gambhir, G. Hangyas-Mihalyne, D. Murray, U. Golebiewska, S. McLaughlin, G. Hangyás-Mihályné, D. Murray, U. Golebiewska, and S. McLaughlin. 2002. Lateral sequestration of phosphatidylinositol 4,5-bisphosphate by the basic effector domain of myristoylated alanine-rich C kinase substrate is due to nonspecific electrostatic interactions. J. Biol. Chem. 277: 34401–34412.

125. Evans, E., and F. Ludwig. 2000. Dynamic strengths of molecular anchoring and material cohesion in fluid biomembranes. J. Phys. Condens. Matter. 12: A315–A320.

126. Stetter, F.W.S., L. Cwiklik, P. Jungwirth, and T. Hugel. 2014. Single lipid extraction: The anchoring strength of cholesterol in liquid-ordered and liquid-disordered phases. Biophys. J. 107: 1167–1175.

127. Tzlil, S., D. Murray, and A. Ben-Shaul. 2008. The "electrostatic-switch" mechanism: Monte Carlo study of MARCKS-membrane interaction. Biophys. J. 95: 1745–1757.

128. Haleva, E., N. Ben-Tal, and H. Diamant. 2004. Increased concentration of polyvalent phospholipids in the adsorption domain of a charged protein. Biophys. J. 86: 2165–2178.

129. Golebiewska, U., A. Gambhir, G. Hangyás-Mihályné, I. Zaitseva, J. Rädler, and S. McLaughlin. 2006. Membrane-bound basic peptides sequester multivalent (PIP2), but not monovalent (PS), acidic lipids. Biophys. J. 91: 588–599.

130. Stahelin, R. V, D. Karathanassis, K.S. Bruzik, M.D. Waterfield, R.L. Williams, W. Cho, J. Bravo, R.L. Williams, W. Cho, and et al Stahelin, R. 2006. Structural and Membrane Binding Analysis of the Phox Homology Domain of Phosphoinositide 3-Kinase-C2 ⌴ * □. J. Biol. Chem. 281: 39396–39406.

131. Hartmann, W., H.-J. Galla, and E. Sackmann. 1977. Direct evidence of charge-induced lipid domain structure in model membranes. FEBS Lett. 78: 169–172.

132. Calabrese, B., M.S. Wilson, S. Halpain, B. Calabrese, S. Margaret, and S. Halpain. 2010. Development and Regulation of Dendritic Dendritic Spines : What Are They ? : 38–47.

133. Sackmann, E. 2015. How actin/myosin crosstalks guide the adhesion, locomotion and polarization of cells. : 3132–3142.

134. Khelashvili, G., H. Weinstein, and D. Harries. 2008. Protein diffusion on charged membranes: a dynamic mean-field model describes time evolution and lipid reorganization. Biophys. J. 94: 2580–2597.

135. Denisov, G., S. Wanaski, P. Luan, M. Glaser, and S. McLaughlin. 1998. Binding of basic peptides to membranes produces lateral domains enriched in the acidic lipids phosphatidylserine and phosphatidylinositol 4,5-biphosphate: An electrostatic model and experimental results. Biophys. J. 74: 731–744.

136. May, S., D. Harries, and A. Ben-Shaul. 2002. Macroion-induced compositional instability of binary fluid membranes. Phys. Rev. Lett. 89: 268102–268105.

137. Grosberg, A.Y., T.T. Nguyen, and B.I. Shklovskii. 2002. Colloquium: The physics of charge inversion in chemical and biological systems. Mod. Rev. Phys. 74: 329–345.

138. May, S., D. Harries, and A. Ben-Shaul. 2000. Lipid Demixing and Protein-Protein Interactions in the Adsorption of Charged Proteins on Mixed Membranes. Biophys. J. 79: 1747–1760.

139. deHaseth, P.L., T.M. Lohman, and M.T. Record. 1977. Nonspecific interaction of lac repressor with DNA: an association reaction driven by counterion release. Biochemistry. 16: 4783–4790.

140. Record, J.M.T., C.F. Anderson, and T.M. Lohman. 1978. Thermodynamic analysis of ion association or release, screening, and ion effects on water activity. Q. Rev. Biophys. 11: 103–178.

141. Rädler, J.O., I. Koltover, A. Jamieson, T. Salditt, and C.R. Safinya. 1997. Structure of DNA-cationic liposome complexes: DNA intercalation in multilamellar membranes in distinct interhelical packing regimes. Science (80-.). 275: 810–814.

142. Koltover, I., T. Salditt, J.O. Rädler, and C.R. Safinya. 1998. An inverted hexagonal phase of cationic liposome-DNA complexes related to DNA release and delivery. Science (80-.). 281: 78–81.

143. Safinya, C.R. 2001. Structures of lipid-DNA complexes: supramolecular assembly and gene delivery. Curr. Opin. Struct. Biol. 11: 440–448.

144. Wagner, K., D. Harries, S. May, V. Kahl, J.O. Rädler, and A. Ben-Shaul. 2000. Counterion release upon cationic lipid-DNA complexation. Langmuir. 16: 303–306.

145. Harries, D., S. May, and A. Ben-Shaul. 2013. Counterion release in membrane–biopolymer interactions. Soft Matter. 9: 9268.

146. Träuble, H. 1971. The movement of molecules across lipid membranes: A molecular theory. J. Membr. Biol. 4: 193–208.

147. Frye, L.D., and M. Edidin. the Rapid Intermixing of Cell Surface Antigens After Formation of Mouse-. : 319–336.

148. Träuble, H., and E. Sackmann. 1971. Studies of the crystalline-liquid crystalline phase transition of lipid model membranes: III. Structure of a steroid-lecithin system below and above the lipid phase transiotion. J. Am. Chem. Soc. 115: 4499–4510.

149. Devaux, P., and H. McConnell. 1972. Lateral Diffusion in Spin-Labeled Phosphatidylcholine Multilayers. J. Am. Chem. Soc. 94: 4475–4481.

150. Galla, H.J., W. Hartmann, U. Theilen, and E. Sackmann. 1979. On two-dimensional passive random walk in lipid bilayers and fluid pathways in biomembranes. J. Membr. Biol. 48: 215–236.

151. Almeida, P.F.F., and W.L.C. Vaz. 1995. Lateral Diffusion in Membranes. In: Lipowsky R, E Sackmann, editors. Handbook f Biological Physics: Structure and Dynamics of Membranes. Amsterdam: Elsevier. pp. 305–358.

152. Saxton, M.J. 2008. A Biological Interpretation of Transient Anomalous Subdiffusion. II. Reaction Kinetics. Biophys. J. 94: 760–771.

153. Schütz, G.J., G. Kada, V.P. Pastushenko, and H. Schindler. 2000. Properties of lipid microdomains in a muscle cell membrane visualized by single molecule microscopy. EMBO J. 19: 892–901.

154. Schwille, P., and E. Haustein. 2002. Fluorescence Correlation Spectroscopy: A Tutorial for the Biophysics Textbook Online (BTOL). .

155. Rusu, L., A. Gambhir, S. McLaughlin, and J. Rädler. 2004. Fluorescence correlation spectroscopy studies of peptide and protein binding to phospholipid vesicles. Biophys. J. 87: 1044–1053.

156. Saffman, P.G., and M. Delbruck. 1975. Brownian motion in biological membranes. Proc Natl Acad Sci USA. 72: 3111–3113.

157. Evans, E., and E. Sackmann. 1988. Translational and rotational drag coefficients for a disk moving in a liquid membrane associated with a rigid substrate. J. Fluid Mech. 194: 553–561.

158. Merkel, R., E. Sackmann, and E. Evans. 1989. Molecular friction and epitactic coupling between monolayers in supported bilayers. J. Phys. 50: 1535–1555.

159. Komura, S., S. Ramachandran, and K. Seki. 2012. Anomalous lateral diffusion in a viscous membrane surrounded by viscoelastic media. EPL (Europhysics Lett. 97: 68007.

160. Tu, K., D.J. Tobias, and M.L. Klein. 1995. Constant pressure and temperature molecular dynamics simulation of a fully hydrated liquid crystal phase dipalmitoylphosphatidylcholine bilayer. Biophys. J. 69: 2558–2562.

161. König, S., and E. Sackmann. 1996. Molecular and collective dynamics of lipid bilayers. Curr. Opin. Colloid Interface Sci. 1: 78–82.

162. Israelachvili, J.N., and H. Wennerström. 1990. Hydration or steric forces between between amphiphilic surfaces? Langmuir. 6: 873–876.

163. Sackmann, E. 1983. Physical foundations of the molecular organization and dynamics of membranes. In: Hoppe W, W Lohmann, H Markl, H Ziegler, editors. Biophysics. Berlin: Springer. pp. 425–457.

164. Kapitza, H.G., D. a Rüppel, H.J. Galla, and E. Sackmann. 1984. Lateral diffusion of lipids and glycophorin in solid phosphatidylcholine bilayers. The role of structural defects. Biophys. J. 45: 577–87.

165. Schneider, M.B., W.K. Chan, and W.W. Webb. 1983. Fast diffusion along defects and corrugations in phospholipid P beta, liquid crystals. Biophys. J. 43: 157–65.

166. Heinemann, S.H., F. Conti, W. Stuhmer, and E. Neher. 1987. Effects of hydrostatic presure on membrane processes: Sodium channels, clcium channels, and exocytosis. J Gen Physiol. 90: 765–778.

167. Grainger, D.W., a. Reichert, H. Ringsdorf, and C. Salesse. 1989. An enzyme caught in action: Direct imaging of hydrolytic function and domain formation of phospholipase A2 in phosphatidylcholine monolayers. FEBS Lett. 252: 73–82.

168. Gallaher, J., K. Wodzińska, T. Heimburg, and M. Bier. 2010. Ion-channel-like behavior in lipid bilayer membranes at the melting transition. Phys. Rev. E - Stat. Nonlinear, Soft Matter Phys. 81: 1–5.

169. Hübner, S., a D. Couvillon, J. a Käs, V. a Bankaitis, R. Vegners, C.L. Carpenter, and P. a Janmey. 1998. Enhancement of phosphoinositide 3-kinase (PI 3-kinase) activity by membrane curvature and inositol-

phospholipid-binding peptides. Eur. J. Biochem. 258: 846–53.

170. Renard, H.-F., M. Simunovic, J. Lemière, E. Boucrot, M.D. Garcia-Castillo, S. Arumugam, V. Chambon, C. Lamaze, C. Wunder, A.K. Kenworthy, A. a. Schmidt, H.T. McMahon, C. Sykes, P. Bassereau, and L. Johannes. 2015. Endophilin-A2 functions in membrane scission in clathrin-independent endocytosis. Nature. 517: 493–6.

171. Bhatia, V.K., K.L. Madsen, P.-Y. Bolinger, A. Kunding, P. Hedegård, U. Gether, and D. Stamou. 2009. Amphipathic motifs in BAR domains are essential for membrane curvature sensing. EMBO J. 28: 3303–3314.

172. Nelson, D.R., and L. Peliti. 1987. Fluctuations in membranes with crystalline and hexatic order. J. Phys. 48: 1085–1092.

173. Helfrich, W. 1978. Steric interactions of fluid membranes in multilayer systems. Z. Naturforsch.A. 33: 305–315.

174. de Gennes, P.G., and J. Prost. 1995. The physics of liquid crystals. Oxford: Oxford University Press.

175. Seifert, U., and R. Lipowsky. 1995. Morphology of vesicles. In: Lipowsky R, E Sackmann, editors. Structure and Dynamics of Membranes. Amsterdam: Elsevier. pp. 403–463.

176. Käs, J., and E. Sackmann. 1991. Shape transitions and shape stability of giant phospholipid vesicles in pure water induced by area-to-volume changes. Biophys. J. 60: 825–44.

177. Mutz, M., and D. Bensimon. 1991. Observation of toroidal vesicles. Phys. Rev. A. 43: 4525–4527.

178. Sackmann, E., and A.-S. Smith. 2014. Physics of cell adhesion: some lessons from cell-mimetic systems. Soft Matter. 10: 1644.

179. Jülicher, F., U. Seifert, and R. Lipowsky. 1993. Phase diagrams and shape transformations of toroidal vesicles. J. Phys. II. 3: 1681–1705.

180. Nelson, P., T. Powers, and U. Seifert. 1995. Dynamical theory of the pearling instability in cylindrical vesicles. Phys. Rev. Lett. 74: 3384–3387.

181. Svetina, S., and B. Zeks. 1989. Membrane bending energy and shape determination of phospholipid vesicles and red blood cells. Eur. Biophys. J. 17: 101–111.

182. Evans, E. a. 1974. Bending resistance and chemically induced moments in membrane bilayers. Biophys. J. 14: 923–931.

183. Häckl, W., U. Seifert, and E. Sackmann. 1997. Effects of fully and partially solubilized amphiphiles on bilayer bending stiffness and temperature dependence of the effective tension of giant vesicles. J. Phys. II. 7: 1141–1157.

184. Deuling, H.J., and W. Helfrich. 1976. Red blood cell shapes as explained on the basis of curvature elasticity. Biophys. J. 16: 861–868.

185. Góźdź, W., and G. Gompper. 1999. Shapes and shape transformations of two-component membranes of complex topology. Phys. Rev. E. 59: 4305–4316.

186. Stokke, B.T., a Mikkelsen, and a Elgsaeter. 1986. Spectrin, human erythrocyte shapes, and mechanochemical properties. Biophys. J. 49: 319–327.

187. Peterson, M.A. 1985. Shape dynamics of nearly spherical membrane bounded fluid cells. Mol. Cryst. Liq. Cryst. 127: 257–272.

188. Peterson, M. 1992. Linear response of the human erythrocyte to mechanical stress. Phys. Rev. A. 45: 4116–4131.

189. Engelhardt, H., and E. Sackmann. 1988. On the measurement of shear elastic moduli and viscosities of erythrocyte plasma membranes by transient deformation in high frequency electric fields. Biophys. J. 54: 495–508.

190. Fischer, T.M., M. Stöhr-Lissen, and H. Schmid-Schönbein. 1978. The red cell as a fluid droplet: tank tread-like motion of the human erythrocyte membrane in shear flow. Science. 202: 894–896.

191. Mukhopadhyay, R., G. Lim H W, and M. Wortis. 2002. Echinocyte shapes: bending, stretching, and shear determine spicule shape and spacing. Biophys. J. 82: 1756–1772.

192. Evans, E., and R. Skalak. 1980. Mechanics and Thermodynamics of Biomembranes. Boca Raton: CRC Press.

193. Brochard, F., and L.J. F. 1975. Frequency spectrum of the flicker phenomenon in erythrocytes. J. Phys.

Fr. 36: 1035–1047.

194. Helfrich, W., and R.M. Servuss. 1984. Undulations, steric interaction and cohesion of fluid membranes. Nuovo Cim. D. 3: 137–151.

195. Albersdorfer, A., T. Feder, and E. Sackmann. 1997. Adhesion-induced domain formation by interplay of long-range repulsion and short-range attraction force: a model membrane study. Biophys. J. 73: 245–257.

196. Rädler, J.O., T.J. Feder, H.H. Strey, and E. Sackmann. 1995. Fluctuation analysis of tension-controlled undulation forces between giant vesicles and solid substrates. Phys. Rev. E. 51: 4526–4536.

197. Evans, E., and W. Rawicz. 1990. Entropy-driven tension and bending elasticity in condensed-fluid membranes. Phys. Rev. Lett. 64: 2094–2097.

198. Lipowsky. 1986. Unbinding Transition of Ineracting Membranes. Prl. : 2541–2544.

199. Zilker, A., H. Engelhardt, and E. Sackmann. 1987. Dynamic reflection interference contrast (RICM) microscopy : a new method to study surface excitations of cells and to measure membrane bending elastic -moduli. 48: 2139–2151.

200. Milner, S.T., and S.A. Safran. 1987. Dynamical fluctuations of droplet microemulsions and vesicles. Phys. Rev. A. 36: 4371–4379.

201. Ben-Isaac, E., Y. Park, G. Popescu, F.L.H. Brown, N.S. Gov, and Y. Shokef. 2011. Effective Temperature of Red-Blood-Cell Membrane Fluctuations. Phys. Rev. Lett. 106: 238103.

202. Strey, H., M. Peterson, and E. Sackmann. 1995. Measurement of erythrocyte membrane elasticity by flicker eigenmode decomposition. Biophys. J. 69: 478–488.

203. Auth, T., S. Safran, and N. Gov. 2007. Fluctuations of coupled fluid and solid membranes with application to red blood cells. Phys. Rev. E. 76: 051910.

204. Bitler, A., and R. Korenstein. 2004. Nano-scale fluctuations of red blood cell membranes reveal nonlinear dynamics. Biophys. J. 86: 582A.

205. Monzel, C., D. Schmidt, C. Kleusch, D. Kirchenbüchler, U. Seifert, A.-S. Smith, K. Sengupta, and R. Merkel. 2015. Measuring fast stochastic displacements of bio-membranes with dynamic optical displacement spectroscopy. Nat. Commun. 6: 8162.

206. Manneville, J.B., P. Bassereau, S. Ramaswamy, and J. Prost. 2001. Active membrane fluctuations studied by micropipet aspiration. Phys. Rev. E. Stat. Nonlin. Soft Matter Phys. 64: 021908.

207. Zidovska, A., and E. Sackmann. 2006. Brownian Motion of Nucleated Cell Envelopes Impedes Adhesion. Phys. Rev. Lett. 96: 048103.

208. May, S., and A. Ben-Shaul. 1995. Spontaneous curvature and thermodynamic stability of mixed amphiphilic layers. J. Chem. Phys. 103: 3839–3848.

209. I. Szleifer, D. Kramer, A. Ben-Shaul, D. Roux, W.M.W.M. Gelbart, I. Szleifer, D. Kramer, A. Ben-Shaul, D. Roux, and W.M.W. ~M. Gelbart. 1988. Curvature Elasticity of Pure and Mixed Surfactant Films. Phys. Rev. Lett. 60: 1966–1969.

210. Szleifer, I., D. Kramer, A. Ben-Shaul, W.M. Gelbart, and S.A. Safran. 1990. Molecular theory of curvature elasticity in surfactant films. J. Chem. Phys. 92: 6800–6817.

211. Parsegian, V. a, N. Fuller, and R.P. Rand. 1979. Measured work of deformation and repulsion of lecithin bilayers. Proc. Natl. Acad. Sci. U. S. A. 76: 2750–2754.

212. Bell, G.I. 1978. Models for the specific adhesion of cells to cells. Science. 200: 618–627.

213. Bell, G.I., M. Dembo, and P. Bongrand. 1984. Cell adhesion Competition Between Nonspecific Repulsion and Specific Bonding. 45.

214. Hatta, K., and M. Takeichi. 1986. Expression of N-cadherin adhesion molecules associated with early morphogenetic events in chick development. Nature. 320: 447–449.

215. Steinberg, M.S. 1975. Adhesion-guided multicellular assembly: a commentary upon the postulates, real and imagined, of the differential adhesion hypothesis, with special attention to computer simulations of cell sorting. J. Theor. Biol. 55: 431–443.

216. Foty, R.A., C.M. Pfleger, G. Forgacs, and M.S. Steinberg. 1996. Surface tensions of embryonic tissues predict their mutual envelopment behavior. 1620: 1611–1620.

217. Katsamba, P., K. Carroll, G. Ahlsen, F. Bahna, J. Vendome, S. Posy, M. Rajebhosale, S. Price, T.M.

Jessell, a Ben-Shaul, L. Shapiro, and B.H. Honig. 2009. Linking molecular affinity and cellular specificity in cadherin-mediated adhesion. Proc. Natl. Acad. Sci. U. S. A. 106: 11594–9.

218. Townes P. S. and Holtfreter J. 1955. Directed movements and selective adhesion of embryonic amphibian cells. J. Exp. Zool. 128: 53–120.

219. Douezan, S., K. Guevorkian, R. Naouar, S. Dufour, D. Cuvelier, and F. Brochard-Wyart. 2011. Spreading dynamics and wetting transition of cellular aggregates. Proc. Natl. Acad. Sci. U. S. A. 108: 7315–20.

220. Seifert, U., and R. Lipowsky. 1990. Adhesion of vesicles. Phys. Rev. A. 42: 4768–4771.

221. Bruinsma, R., A. Behrisch, and E. Sackmann. 2000. Adhesive switching of membranes: Experiment and theory. Phys. Rev. E. 61: 4253–4267.

222. Evans, E. 1995. Chapter 15 Physical actions in biological adhesion. Handb. Biol. Phys. 1: 723–754.

223. Cinamon, G., V. Shinder, and R. Alon. 2001. Shear forces promote lymphocyte migration across vascular endothelium bearing apical chemokines. Nat.Immunol. 2: 515–522.

224. Smith, A.-S., E. Sackmann, and U. Seifert. 2004. Pulling Tethers from Adhered Vesicles. Phys. Rev. Lett. 92: 1–4.

225. Nardi, J., R. Bruinsma, and E. Sackmann. 1998. Adhesion-induced reorganization of charged fluid membranes. Phys. Rev. E. 58: 6340–6354.

226. Simson, R., E. Wallraff, J. Faix, J. Niewöhner, G. Gerisch, and E. Sackmann. 1998. Membrane bending modulus and adhesion energy of wild-type and mutant cells of Dictyostelium lacking talin or cortexillins. Biophys. J. 74: 514–22.

227. Bakhti, M., N. Snaidero, D. Schneider, S. Aggarwal, W. Möbius, A. Janshoff, M. Eckhardt, K.-A. Nave, and M. Simons. 2013. Loss of electrostatic cell-surface repulsion mediates myelin membrane adhesion and compaction in the central nervous system. Proc. Natl. Acad. Sci. U. S. A. 110: 3143–8.

228. Hu, Y., I. Doudevski, D. Wood, M. Moscarello, C. Husted, C. Genain, J.A.A. Zasadzinski, and J. Israelachvili. 2004. Synergistic interactions of lipids and myelin basic protein. Proc. Natl. Acad. Sci. U. S. A. 101: 13466–71.